PL-TR-94-2295 SSS-DPR-94-14828

Analyses of the Seismic Characteristics of U.S. and Russian Cavity Decoupled Explosions

J. R. Murphy
I. O. Kitov
J. L. Stevens
D. D. Sultanov
B. W. Barker
N. Rimer
M. C. Friedman

Maxwell Laboratories, Incorporated
S-CUBED Division
P. O. Box 1620
La Jolla, CA 92038-1620

November, 1994

Scientific Report No. 1

PHILLIPS LABORATORY
Directorate of Geophysics
AIR FORCE MATERIEL COMMAND
HANSCOM AFB, MA 01731-3010

SPONSORED BY
Advanced Research Projects Agency (DoD)
Nuclear Monitoring Research Office
ARPA ORDER No. A-128

MONITORED BY
Phillips Laboratory
CONTRACT No. F19628-93-C-0126

This technical report has been reviewed and is approved for publication.

JAMES F. LEWKOWICZ
Contract Manager
Earth Sciences Division

JAMES F. LEWKOWICZ
Director
Earth Sciences Division

This report has been reviewed by the ESC Public Affairs Office (PA) and is releasable to the National Technical Information Service (NTIS).

Qualified requestors may obtain additional copies from the Defense Technical Information Center. All others should apply to the National Technical Information Service.

If your address has changed, or if you wish to be removed from the mailing list, or if the addressee is no longer employed by your organization, please notify PL/IM, 29 Randolph Road, Hanscom AFB, MA 01731-3010. This will assist us in maintaining a current mailing list.

Do not return copies of this report unless contractual obligations or notices on a specific document requires that it be returned.

REPORT DOCUMENTATION PAGE

Form Approved
OMB No. 0704-0188

1. AGENCY USE ONLY *(Leave blank)*	2. REPORT DATE	3. REPORT TYPE AND DATES COVERED
	November, 1994	Scientific No. 1

4. TITLE AND SUBTITLE

Analyses of the Seismic Characteristics of U.S. and Russian Cavity Decoupled Explosions

5. FUNDING NUMBERS

Contract:
F19628-93-C-0126
PE 62301E
PR NM93 TA GM
WUAJ

6. AUTHOR(S)

J. R. Murphy, I. O. Kitov*, J. L. Stevens, D. D. Sultanov*, B. W. Barker, N. Rimer, M. C. Friedman

7. PERFORMING ORGANIZATION NAME(S) AND ADDRESS(ES)

Maxwell Laboratories, Inc.
S-CUBED Division
P.O. Box 1620
La Jolla, CA 92038-1620

8. PERFORMING ORGANIZATION REPORT NUMBER

SSS-DPR-94-14828

9. SPONSORING/MONITORING AGENCY NAME(S) AND ADDRESS(ES)

Phillips Laboratory
29 Randolph Road
Hanscom AFB, MA 01731-3010

Contract Manager: James F. Lewkowicz/GPEH

10. SPONSORING/MONITORING AGENCY REPORT NUMBER

PL-TR-94-2295

11. SUPPLEMENTARY NOTES

*Institute for Dynamics of the Geospheres, Russian Academy of Sciences

12a. DISTRIBUTION/AVAILABILITY STATEMENT

Approved for public release; distribution unlimited

12b. DISTRIBUTION CODE

13. ABSTRACT *(Maximum 200 words)*

This report presents a summary of the initial results of an on-going joint research program in which S-CUBED scientists are working with Russian scientists from the Institute for Dynamics of the Geospheres in an attempt to develop a better understanding of the effects of cavity decoupling on the seismic signals produced by underground nuclear explosions. This program includes analyses of seismic data recorded from a series of 10 tamped and 12 decoupled HE tests which were conducted in cavities of different sizes and shapes in Kirghizia in 1960, a theoretical evaluation of the influence of radiation diffusion effects on nuclear cavity decoupling efficiency and an analysis of data recorded from six small (0.01 to 0.50 kt) Russian nuclear tests conducted in a 32 m radius, water-filled cavity in salt at the Azgir test site.

14. SUBJECT TERMS

Seismic, Explosion, Kirghizia, HE, Cavity Decoupling, Nuclear, Azgir, Radiation

15. NUMBER OF PAGES

64

16. PRICE CODE

17. SECURITY CLASSIFICATION OF REPORT	18. SECURITY CLASSIFICATION OF THIS PAGE	19. SECURITY CLASSIFICATION OF ABSTRACT	20. LIMITATION OF ABSTRACT
Unclassified	Unclassified	Unclassified	Unlimited

CLASSIFIED BY:
DECLASSIFY ON:

Table of Contents

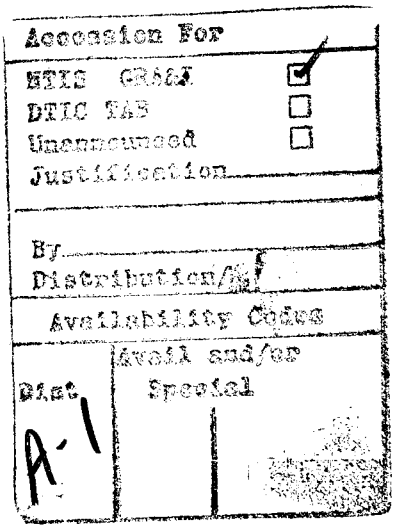

List of Illustrations

1. INTRODUCTION

It has long been recognized that the most effective means for evading the detection of a clandestine underground nuclear test is to detonate the explosion in a cavity which is large enough to substantially decouple the radiated seismic signal. However, despite the fact that some 35 years have now elapsed since the public introduction of this evasion concept at the Nuclear Test Ban Conference in Geneva (Latter, 1959), a number of major issues of importance with respect to seismic monitoring still remain unresolved. By definition, a fully decoupled explosion is one in which the cavity wall experiences no significant nonlinear deformation and, consequently, the seismic radiation from such an explosion can be readily estimated using linear, elastic wave theory. However, the cavities required to achieve such full decoupling are very large (i.e. on the order of $1 \times 10^5 m^3$/kiloton) and difficult to construct and, therefore, there is a significant incentive to quantitatively evaluate the penalties associated with using progressively smaller cavities. Of course, as the cavity radius is decreased at a given yield, the decoupling becomes only partial and the problem of estimating the seismic radiation is greatly complicated by the attendant nonlinear wall response. Similar considerations apply to the effects of departures from spherical cavity shape. From an engineering perspective, it is often easier to construct elongated cavities than to construct a spherical cavity of the same volume and, in fact, most large solution cavities in salt are more nearly ellipsoidal than spherical. Once again, if the cavity is large enough that the response of the cavity wall is effectively linear, then the solution for the radiated seismic wavefield can be estimated using conventional elastic wave theory. However, if significant nonlinearity is induced by the explosion, the seismic coupling efficiency can only be properly addressed using sophisticated, multi-dimensional finite difference codes.

Over the past several years, we at S-CUBED have been carrying out a wide range of nonlinear, finite difference simulations of cavity decoupling in which the effects of cavity size and shape have been analyzed for explosions in salt, granite and dry tuff source media (Murphy *et al.*, 1988; Stevens *et al.*, 1991a, 1991b). These have included one-dimensional simulations of explosions in spherical cavities over a wide range of yield/volume ratios, as well as two-dimensional axisymmetric simulations of explosions of different yields in an ellipsoidal cavity in salt characterized by a 4 to 1 aspect ratio. While the results of these simulations have been very informative, it has been difficult to critically assess their fidelity because of the limited U.S. experimental database on cavity decoupling. However, scientists from the Institute for Dynamics of the Geospheres (IDG) of the Russian Academy of Sciences have recently begun publishing new information on some Russian cavity decoupling experiments (e.g., Adushkin *et al.*, 1992) which can provide data relevant to these issues. In this report, we summarize the initial results of a joint S-CUBED/IDG research investigation which has the objective of integrating these newly available data and theoretical results in an attempt to validate a quantitative prediction capability which can be used by the seismic verification community to evaluate the plausibility of various cavity decoupling evasion scenarios.

This report is organized around three main topical areas, each of which is addressed separately in the following three sections. In Section 2, an extensive Russian HE cavity decoupling test series which was conducted in limestone in a mine in Kirghizia in 1960 is described, and seismic data recorded from these tests in cavities of different size and shape are compared and evaluated in a preliminary fashion. This is followed in Section 3 by an analysis of the potential influence of radiation diffusion effects on decoupling efficiency in which the induced seismic motions corresponding to theoretical simulations conducted with and without incorporation of radiation diffusion are systematically compared for a representative range of modeling parameters. The series of six Russian nuclear tests conducted in a water-filled cavity at Azgir is described in detail for the first time in Section 4 where initial samples of the near-regional

seismic data recorded from these tests are presented and compared. Section 5 presents a summary of the current status of these three investigations, as well as some preliminary conclusions based upon the research completed to date.

2. KIRGHIZIA HE DECOUPLING TESTS

During the summer of 1960, the Russians carried out a series of HE cavity decoupling tests in limestone at a site in Kirghizia. The tests were conducted in a uranium mine in the Tywya Mountains, located approximately 70 km east of the city of Fergana at 40.4°N, 72.6°E. These tests were comparable to the corresponding U.S. COWBOY HE decoupling test series which was conducted in salt at about this same time, but were somewhat more comprehensive in that they included a number of charge configurations which were not investigated in the COWBOY series. In particular, the Kirghizia series included tests designed to evaluate the effects of cavity shape and charge emplacement geometry on decoupling effectiveness.

The tests were conducted in chambers which were excavated off of the main mine access tunnel at a depth of about 290 m below the surface. Figure 1 shows vertical sections along the access tunnel and perpendicular to the tunnel at the test location. It can be seen from this figure that the mine penetrates a mesa rather than a mountain and that the surface topography above the tests is relatively smooth over distances on the order of several hundreds of meters from ground zero. The relative locations and configurations of the various explosion chambers which were excavated for this test series are shown in Figure 2 where it can be seen that the maximum separation between any of the tests was less than 150 m. The five excavated decoupling test chambers shown here include three spherical cavities with diameters in the 3.6 to 9.8 m range (i.e., radii of 1.81, 2.88 and 4.92 m), as well as two nonspherical chambers of roughly cylindrical shape encompassing volumes of about 25 m^3. These cavities were excavated in hard, homogeneous limestone characterized by compressional wave velocities in the 5.5 to 6.0 km/sec range.

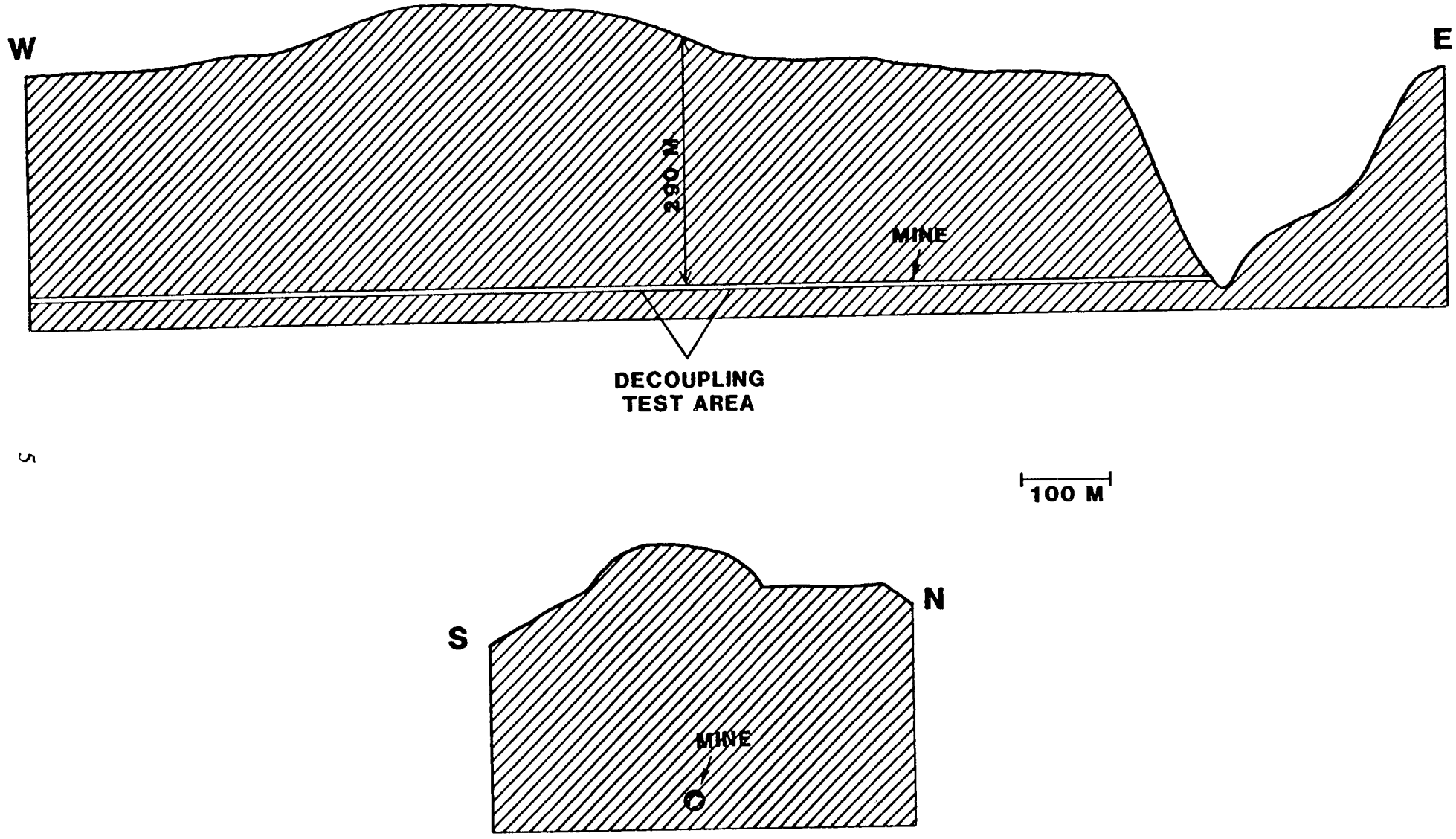

Figure 1. Vertical sections along (top) and perpendicular to (bottom) the mine access tunnel used for the Kirghizia cavity decoupling experiments.

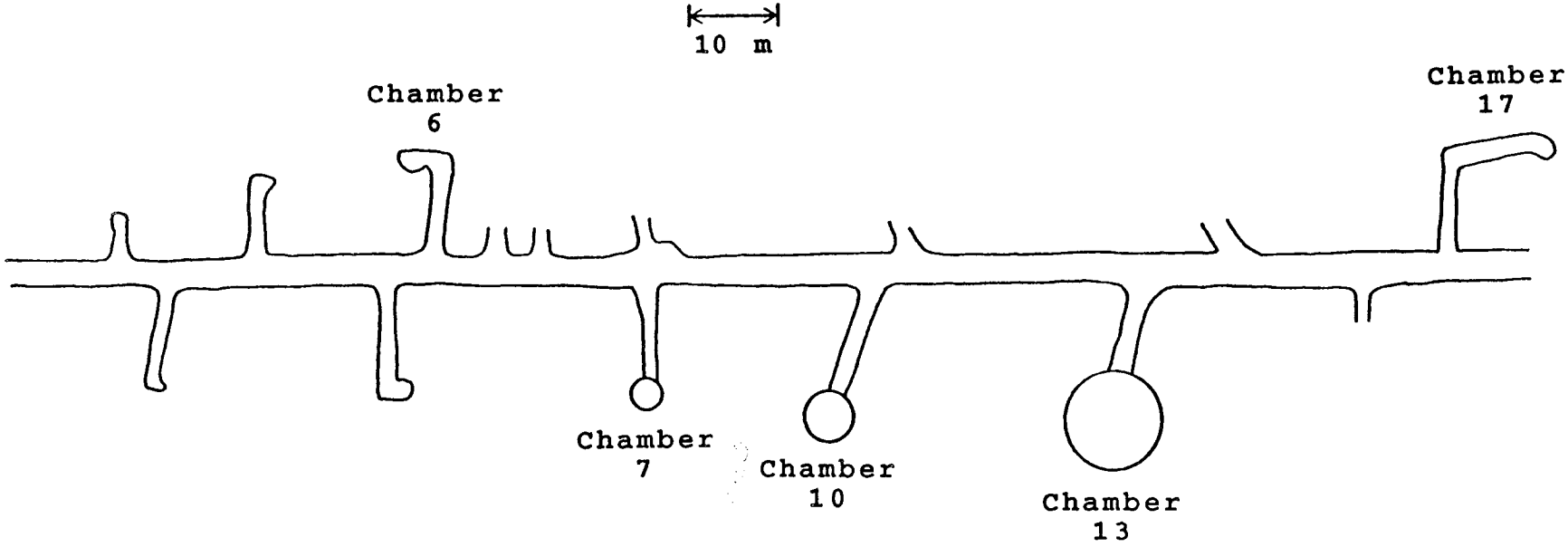

Figure 2. Relative locations and configurations of the various explosion chambers constructed in the Kirghizia limestone mine for the Russian HE decoupling test series.

The test series was composed of 10 tamped and 12 decoupled explosions having yields of 0.1, 1.0 and 6.0 tons. The explosives consisted of ammonium nitrate, except for the two 6.0 ton tests which utilized a mix of TNT and ammonium nitrate. For the cavity tests, the explosives were suspended in the chambers and included cases in which the explosives were positioned in the center of the cavity, as well as cases in which they were positioned off-center, near the cavity walls. The configurations of the various cavity tests are graphically summarized for each of the five test chambers in Figure 3. It can be seen that explosions of varying yield were detonated in two of the chambers (i.e. #10 and #13), thus providing data which can be used to assess the effects of variations in scaled cavity size on decoupling effectiveness.

Seismic data were recorded from these tests at locations in the mine over a distance range extending from about 10 to 250 m from the sources. Most of these data were recorded on broadband velocity (VIB) sensors which were installed in drill holes and niches excavated in the wall of the mine. Peak amplitudes of displacement and velocity have been reported for over 250 of these recording locations and about 60 of the corresponding seismograms have now been digitized at IDG and prepared for detailed spectral analysis. Samples of the radial particle velocity seismograms recorded at a range of about 100 m from one tamped and two cavity decoupled 1.0 ton explosions are shown in Figure 4. It can be seen that these data are of good quality and that they illustrate the expected differences in dominant frequency content between tamped and cavity decoupled explosions of the same yield. That is, because the characteristic seismic source radius is larger for a tamped explosion than for a cavity decoupled explosion of the same yield, the characteristic frequency of the tamped seismic source is expected to be lower, consistent with the observed data of Figure 4. As will be noted in the following discussion, this point has important implications with respect to the interpretation of observed differences in peak amplitude levels between tamped and decoupled explosions.

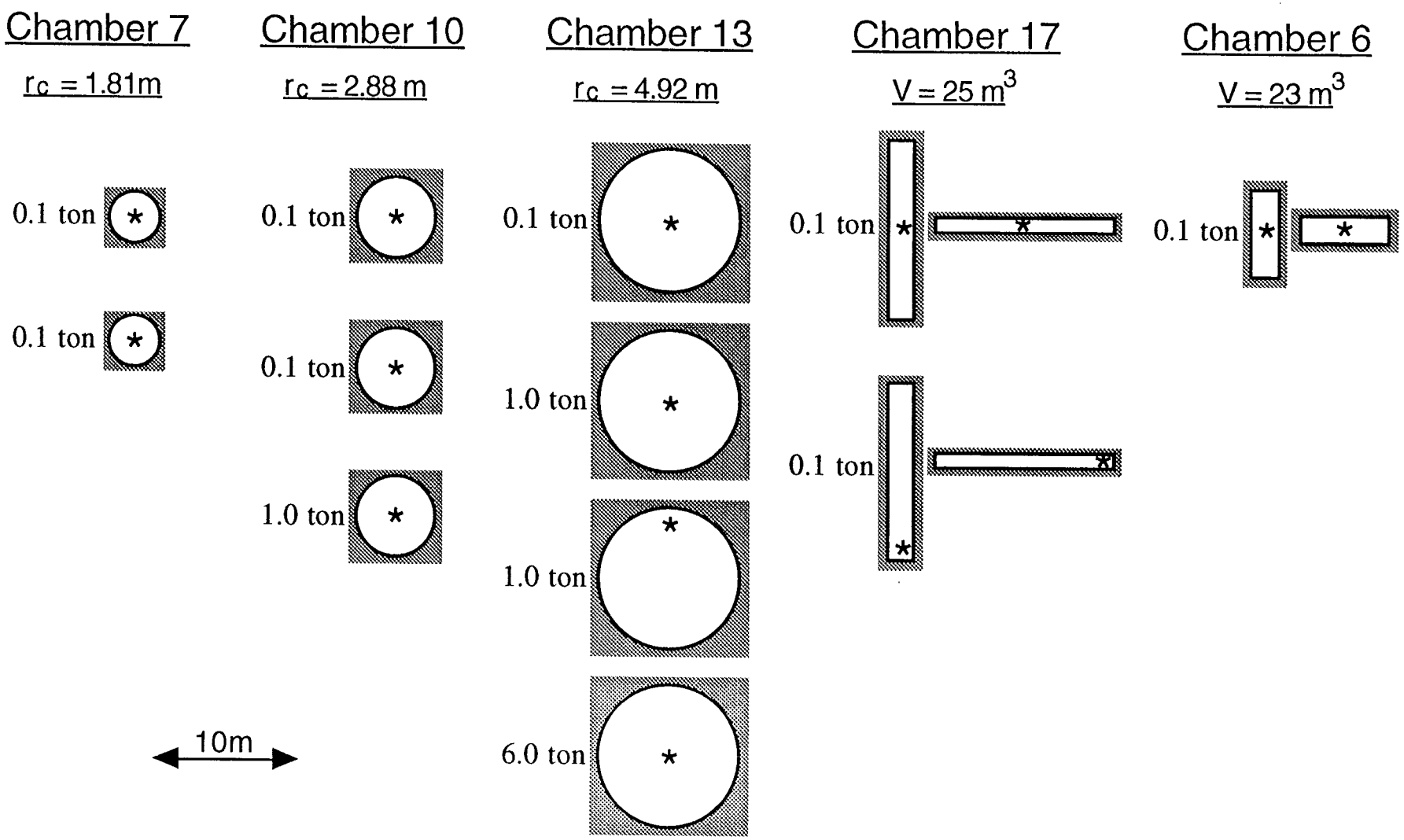

Figure 3. Graphical summary of the HE decoupling tests conducted in each of the excavated explosion chambers. The asterisk denotes the emplacement location of the charge within the chamber for each test. For the nonspherical cases, both horizontal (left) and vertical (right) sections through the chambers are displayed.

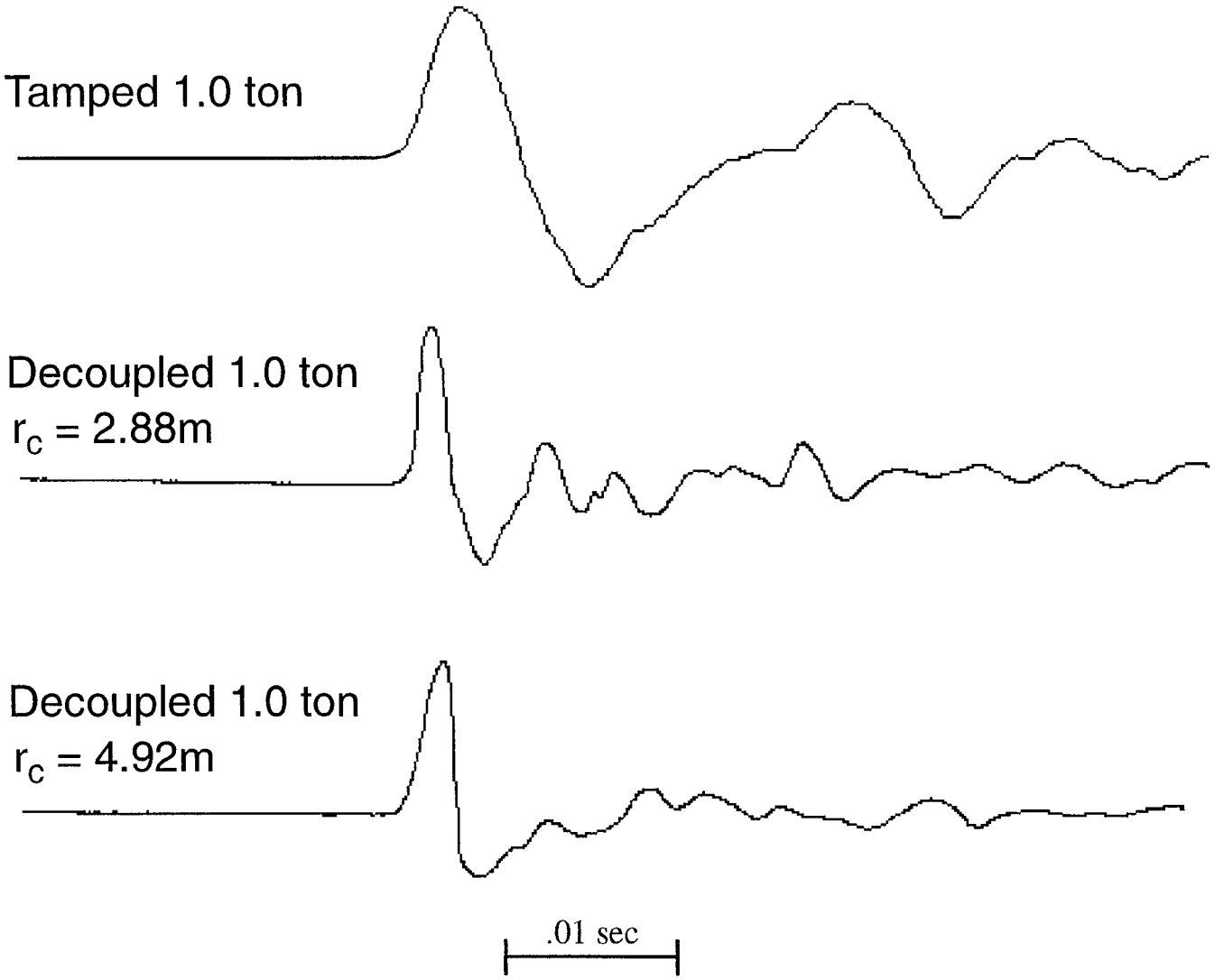

Figure 4. Comparison of radial particle velocity seismograms recorded at a range of about 100m from 1.0 ton tamped and cavity decoupled Kirghizia HE explosions.

The peak displacement data observed from the 0.1, 1.0 and 6.0 ton tamped explosions are plotted as a function of source/receiver distance in Figure 5. Multiple tests were conducted at the 0.1 and 1.0 ton yields and it can be seen that the observed data from these tests are reasonably consistent and that they provide well-constrained average amplitude levels as a function of distance over the range extending from about 10 to 200 m. A least-squares statistical analysis of the extensive 0.1 ton tamped data set gives an average distance decay rate which is approximately proportional to $R^{-1.1}$ over this range. Consequently, the distance attenuation was constrained to be $R^{-1.1}$ in the statistical analyses of the observed data from the 1.0 and 6.0 ton tamped explosions, leading to the three parallel straight line fits to the data shown in Figure 5. It can be seen that all these data are quite consistent with the single, nominal distance attenuation rate.

The analysis of the peak amplitude data recorded from the Kirghizia decoupling test series is still in progress and no definitive results are available at this time. However, some selected, preliminary examples will be presented in the following discussion to illustrate the kinds of issues which are currently under investigation. As the first example, the peak displacement data recorded from one of the 1.0 ton decoupled tests are plotted versus distance in Figure 6 where they are compared with the corresponding tamped 1.0 ton average peak displacement level (solid line) from Figure 5. In this case, the decoupled test was detonated at the center of the 4.92 m radius cavity and the dashed line on Figure 6 denotes the least-squares fit to the observed data from that test, obtained using the same distance attenuation constraint (i.e. $R^{-1.1}$) used in the analysis of the corresponding tamped data. Comparing the levels of the solid and dashed lines, it can be seen that these data are consistent with an average peak displacement decoupling factor of about 10. That is, this cavity test was clearly decoupled, although the observed peak displacement decoupling factor is significantly smaller than the nominal low frequency decoupling factor reported for the U.S. nuclear cavity experiment STERLING. However, as was noted above with reference to Figure 4, the peak

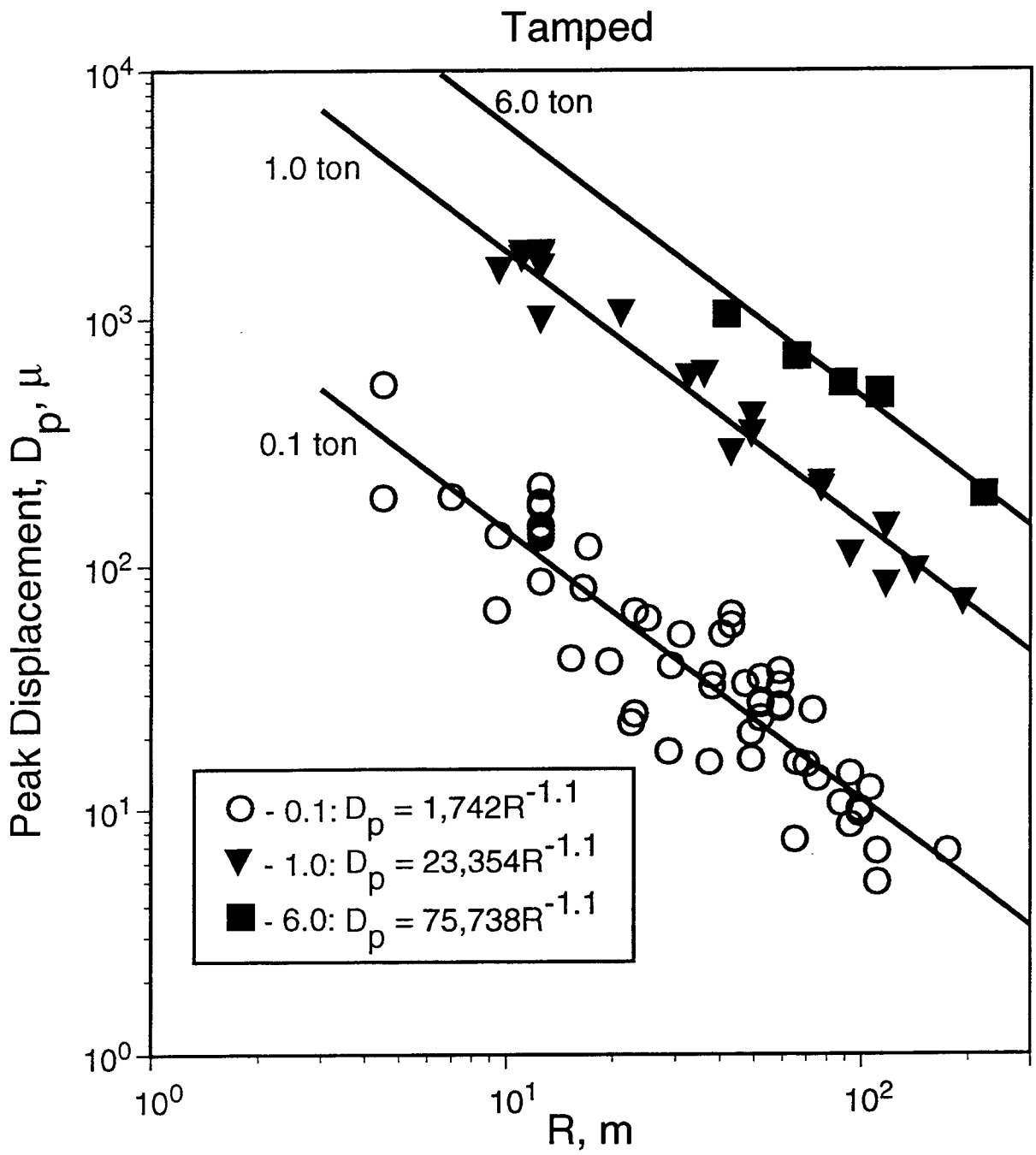

Figure 5. Comparison of peak displacement data observed from the various tamped HE tests which provide the reference base for the decoupling analysis.

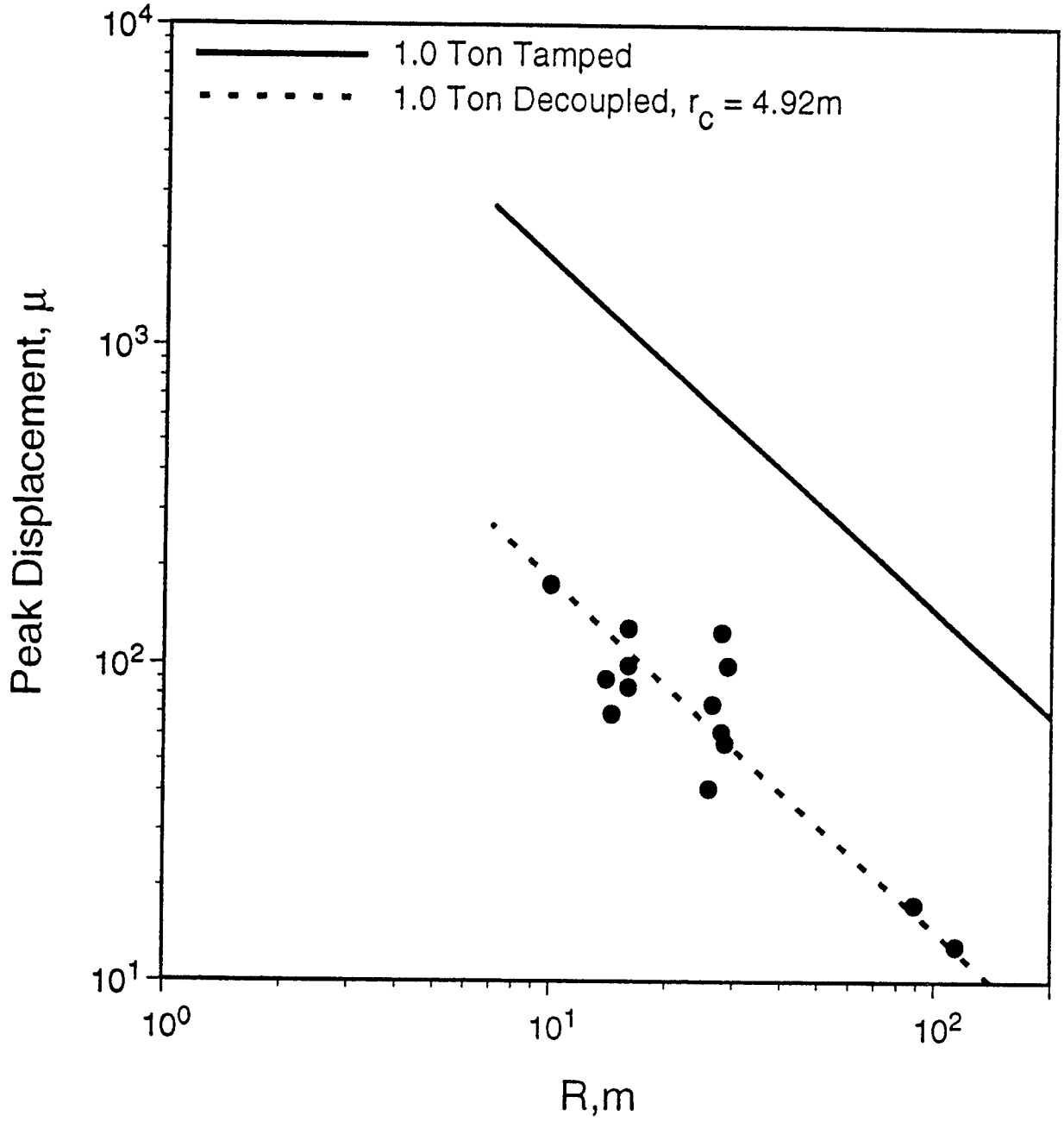

Figure 6. Comparison of peak amplitude levels of displacement as a function of range for 1.0 ton tamped and cavity decoupled explosions.

displacement levels being compared in Figure 6 correspond to very different frequency components and, therefore, can not be interpreted directly in terms of the low frequency decoupling level which is typically used to quantify decoupling efficiency. More detailed spectral analyses of the complete waveform data are required to estimate this latter quantity.

Despite the fact that peak amplitude data are not well suited for establishing absolute levels of decoupling effectiveness, they do provide a rough basis for comparison which can be used to assess relative effects of variables such as cavity size, shape and charge emplacement geometry. That is, while the dominant frequencies of the peak motions corresponding to tamped and cavity decoupled explosions of the same yield are observed to be quite different, those associated with decoupled explosions of the same yield in different cavity configurations are observed to be comparable. Thus, these data can be directly compared to estimate differences in decoupling effectiveness at that common dominant frequency. For example, Figure 7 shows a comparison of the peak displacement data observed from 0.1 ton decoupled tests in the spherical cavities with radii of 1.81 and 2.88 m. It can be seen that the observed peak displacement levels for these two tests appear to be essentially independent of cavity radius over this range of observation. This is not a surprising observation given that the equivalent scaled STERLING cavity radius for this yield and depth of burial is less than 1.5 m. That is, even allowing for uncertainties in the seismic coupling efficiency of the HE source, it appears that both of these tests were fully decoupled and the low frequency decoupling effectiveness is not theoretically predicted to depend on cavity radius under these conditions (Stevens *et al.*, 1991a).

With respect to the influence of cavity shape, Figure 8 shows a comparison of the peak displacement data observed from 0.1 ton decoupled tests in spherical and cylindrical cavities of the same volume (i.e. $25m^3$). In this case, the spherical cavity had a radius of 1.81 m and the nonspherical cavity was roughly cylindrical with a diameter of about 2 m and a length of about 6 m. It can be seen that the data of Figure 8 indicate that the peak

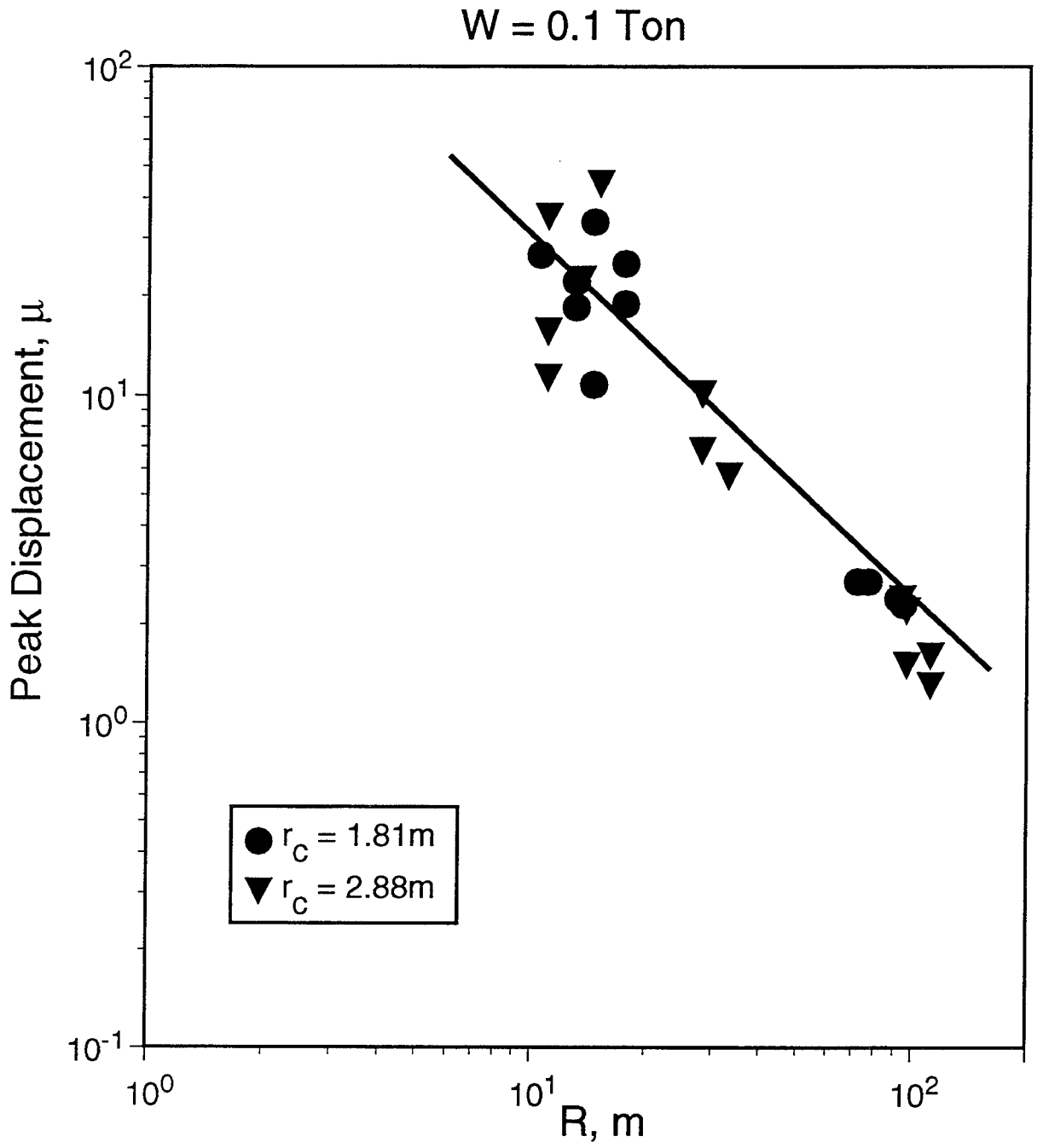

Figure 7. Comparison of peak displacement data observed from 0.1 ton decoupled tests in spherical cavities with radii of 1.81 and 2.88m.

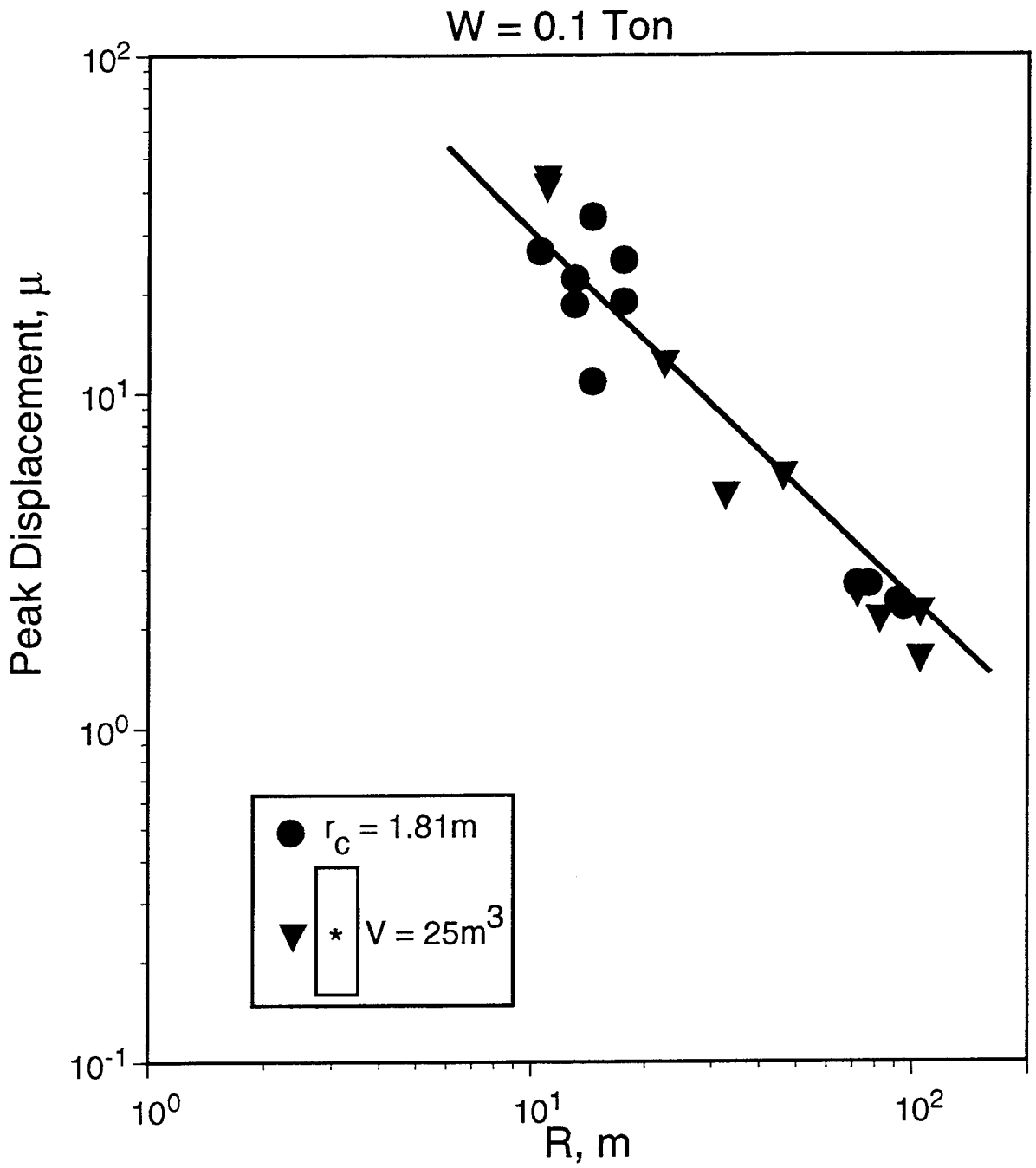

Figure 8. Comparison of peak displacement data observed from 0.1 ton decoupled tests in different shaped cavities having volumes of about 25m^3.

displacement levels associated with these two tests are indistinguishable within the scatter of the data. This suggests that the low frequency decoupling effectiveness is comparable for these two cavity shapes at this yield to volume ratio, which is again in agreement with previous theoretical results. That is, Stevens *et al.* (1991b) conducted detailed, nonlinear finite difference simulations of nuclear detonations in an ellipsoidal (i.e., prolate spheroidal) cavity characterized by an aspect ratio of 4 to 1 and found that the computed low frequency decoupling effectiveness in such a cavity is nearly identical to that estimated for the same explosion in a spherical cavity of the same total volume. It follows that since the equivalent aspect ratio of the cylindrical cavity represented in Figure 8 is smaller (i.e., about 3 to 1) than that considered in this theoretical simulation, it is not surprising that the induced low frequency ground motion levels are essentially the same for the spherical and nonspherical cavities in this case.

The effects of charge emplacement geometry are addressed in Figure 9 which shows a comparison of the peak displacement data observed from two 1.0 ton decoupled tests conducted at different locations in the 4.92 m radius spherical cavity. In this case, one test was carried out with the charge positioned in the center of the cavity, while the other was conducted with the charge centered 1 m from the cavity wall. It can be seen from Figure 9 that the observed peak displacement levels for the test near the cavity wall appear to be somewhat larger on average than those observed from the corresponding test in the center of the cavity. This suggests that the proximity to the cavity wall in the former test resulted in an increase in the degree of nonlinear response in the surrounding medium and, hence, increased seismic coupling efficiency in this case. This suggests that the decoupling effectiveness of the test near the cavity wall is somewhat lower than that of the corresponding test at the center of the cavity. However, the magnitude of the effect appears to be less than a factor of two in this case, at least in the frequency range represented by this peak displacement data.

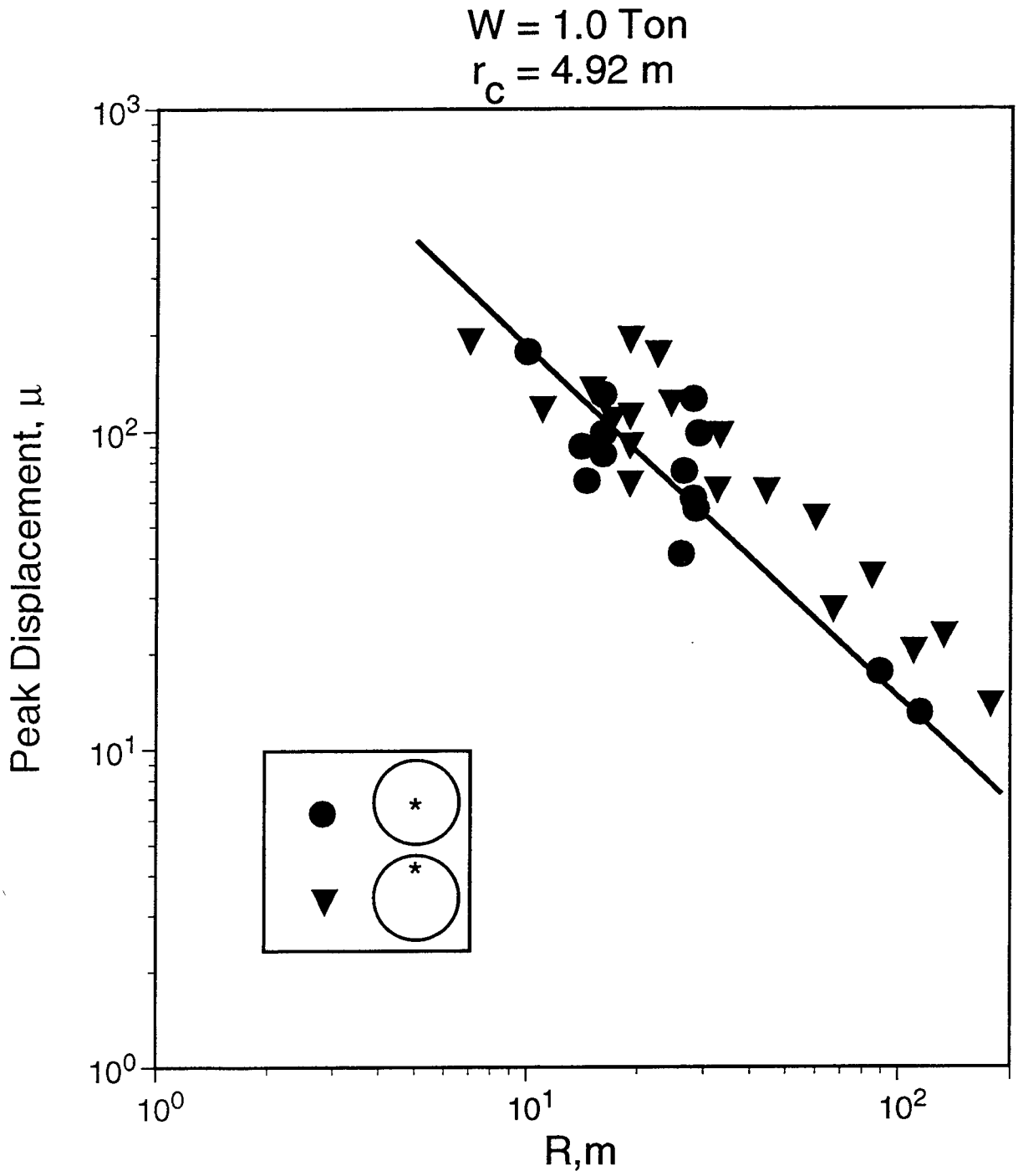

Figure 9. Comparison of peak displacement data observed from 1.0 ton decoupled tests at different locations in the 4.92m radius spherical cavity.

It was noted above that in order to make a fully quantitative assessment of the decoupling effectiveness of the various Kirghizia HE tests, it will be necessary to carry out detailed spectral analyses of the recorded waveform data. Such analyses have recently been initiated and Figure 10 shows some of the preliminary results obtained for the 1.0 ton decoupled tests conducted in the center of the 2.88 m and 4.92 m radius spherical cavities. In this figure, the plotted frequency dependent decoupling factors correspond to the ratios of the spectrum estimated from the ground motions recorded from a tamped 1.0 ton test at a range of 110 m to the spectra estimated from the ground motions recorded at that same distance from the decoupled 1.0 ton tests in the two spherical cavities. It can be seen from this figure that the frequency dependent decoupling factors estimated for these two tests are remarkably consistent over the entire frequency range extending from about 3 to 500 Hz. In particular, they both indicate a maximum low frequency decoupling factor of about 50, in contrast to the apparent peak displacement decoupling ratio of 10 which was documented previously in Figure 6. These observations confirm the fact that peak amplitude data are not suitable for defining the absolute levels of decoupling effectiveness. In any case, the maximum low frequency decoupling factor of 50 shown in Figure 10 is somewhat lower than the nominal low frequency decoupling factor of 70 which is usually cited for the U.S. STERLING nuclear decoupling experiment (OTA, 1988). Spectral analyses of a larger sample of the Kirghizia data will have to be conducted before it can be determined whether this difference is statistically significant and, if so, whether it can be associated with possible differences in seismic source coupling between explosions in limestone and salt.

A final point which needs to be addressed in conjunction with Figure 10 concerns the observed frequency dependence of the decoupling factors for the two 1.0 ton explosions in the different sized spherical cavities. Now the equivalent scaled STERLING cavity radius for this yield and depth of burial is approximately 3 m, which suggests that both these tests were essentially fully decoupled. Therefore, as was noted above in the discussion of the peak amplitude data of Figure 7, the low frequency decoupling

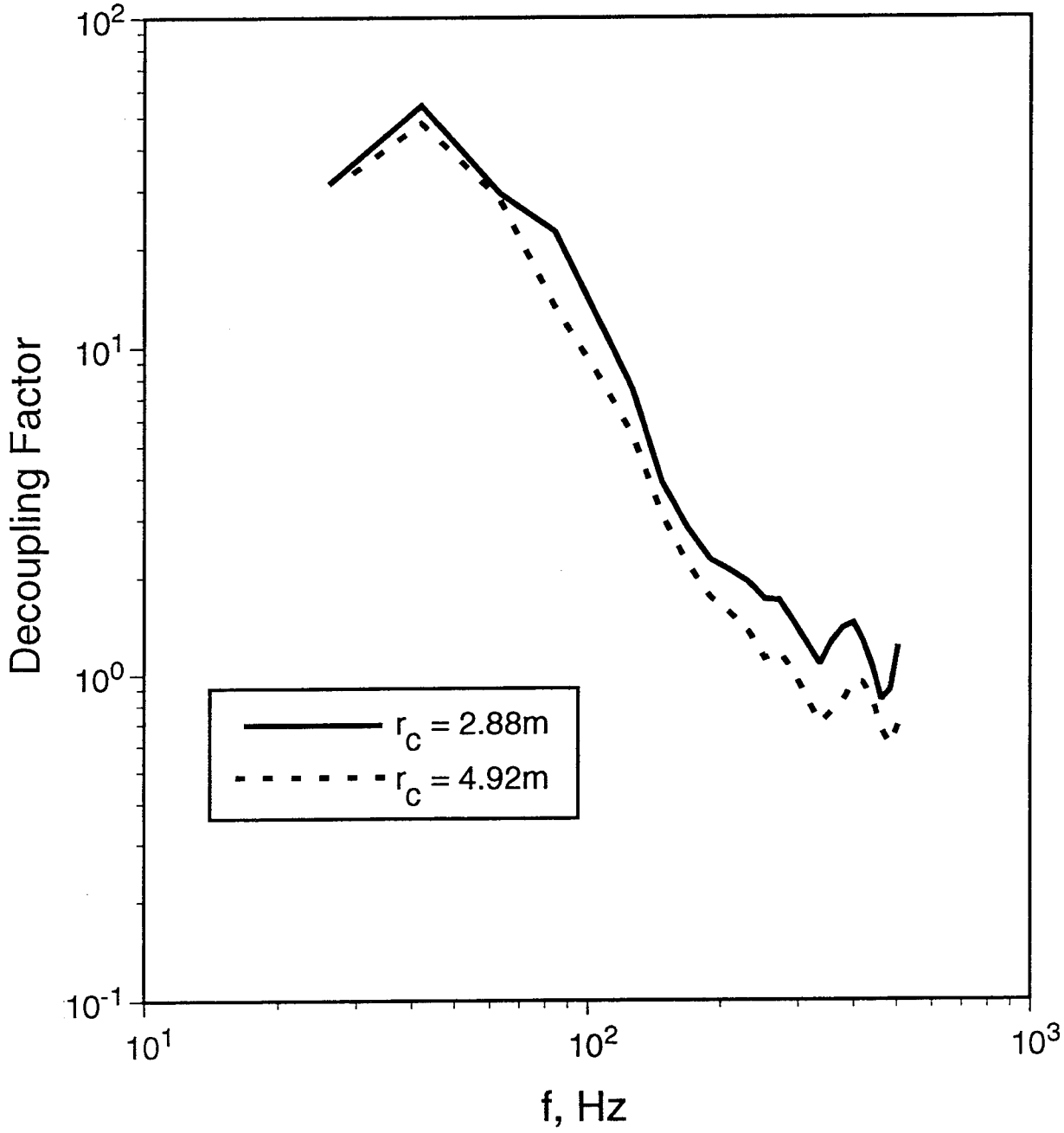

Figure 10. Comparison of the observed frequency dependent decoupling factors for 1.0 ton tests in spherical cavities with radii of 2.88 and 4.92m.

efficiency is theoretically expected to be independent of cavity radius over this range (Stevens *et al.*, 1991a), in agreement with the data of Figure 10. However, this same theoretical model also predicts that the high frequency decoupling effectiveness of the 4.92 m radius cavity should be greater than that of the 2.88 m radius cavity by more than a factor of 2 in this case, and this prediction is not in agreement with the observed high frequency data shown in Figure 10. Again, it will be necessary to analyze a larger sample of these waveform data before it can be determined whether this apparent discrepancy is statistically significant.

In summary, seismic data recorded from an extensive series of HE cavity decoupling experiments in limestone conducted by the Russians in Kirghizia during the summer of 1960 have been collected and digitized and are currently being analyzed in an attempt to develop a better understanding of the effects of variables such as cavity size, shape and charge emplacement geometry on decoupling effectiveness. Preliminary results of the on-going data analysis suggest that the observed effects of decoupling on these peak amplitude and waveform data are generally consistent with both previous experience and the predictions of available theoretical models, although there are some interesting apparent discrepancies which will require further investigation.

3. EVALUATION OF THE EFFECT OF NUCLEAR RADIATION ON SEISMIC DECOUPLING

Glenn and Goldstein (1994) recently suggested that the inclusion of radiation diffusion effects can have a significant influence on the computed seismic source function for cavity decoupled nuclear tests. In order to further investigate this issue, we carried out a series of radiation/hydrodynamic finite difference simulations of a 380 ton nuclear explosion in a 17 m radius air-filled cavity in salt (i.e., STERLING equivalent). The calculations were run both with and without radiation and over a wide range of air opacities.

The calculations were initiated with a 15 cm sphere of aluminum with a density of 2.0 gm/cm^3, containing 380 tons of energy, placed in the center of a 17 m air-filled salt cavity. The density of the air and salt were 0.0012 gm/cm^3 and 2.1417 gm/cm^3, respectively. The ambient air pressure in the cavity was taken to be 1 bar. The air equation of state used in the calculations was that developed by M. Alme at the Air Force Weapons Laboratory in 1977. The gray air opacities, which include carbon, nitrogen, oxygen, neon and argon were taken from the Los Alamos National Laboratories' (LANL) TOPS tables. The aluminum equation of state and gray opacities came from LANL's SESAME and TOPS tables (i.e., SESAME identification number 7282, TOPS identification number 19111). The multifrequency cold air absorption coefficients used to transport radiation from the thick air shock to the walls of the cavity were obtained from SAIC. The multifrequency absorption coefficients in the air window (i.e., 0 to 6 ev) were taken to be 100 cm^2/gm, and uniform with frequency.

In the simulation model, salt extends from the cavity wall at a radius of 17 m to a radius of 500 m, with an initial finite difference zone size of 110 microns at the cavity wall, increasing at greater distances with a zoning ratio of 1.05. As will be discussed below, the adequacy of this zoning has

been tested and verified through comparisons with supplemental calculations which were performed using a much finer grid. Within the cavity, the device was represented by 25 zones with a 0.89 mass-zoning ratio and the air-filled portion was divided into 45 zones with a mass-zoning ratio of 1.5 to a distance of 10 m and 0.85 out to 17 meters. Both the radiation and non-radiation calculations used exactly the same zoning and material properties.

The ZOOS Lagrangian coupled radiation/hydrodynamic code (S-CUBED, 1969) was used for all the calculations. The calculations were performed for a one-dimensional (i.e., spherically symmetric) geometry. The main radiation effects that are modeled in these simulations are the generation of radiation by the source, absorption of radiation by the air, and vaporization of zones of salt close to the cavity wall by the remaining incident radiation. Most of the energy is absorbed close to the device and establishes a high temperature air shock that radiates and propagates outward. The only radiation that survives to reach the cavity wall prior to the arrival of the shock is in the energy range 0-6 ev; all other radiation is absorbed by the hot air shock. The energy in this window amounts to approximately 1% of the 380 tons of source energy.

The results of the calculations are illustrated in Figures 11-14. Figures 11 and 12 show the pressure and impulse versus time at the cavity wall and Figures 13 and 14 show the corresponding pressure and impulse versus time at a distance of 25 m from the center of the cavity (i.e., 8 meters into the salt). The pressure time histories show the reverberations that are characteristic of explosions in air-filled cavities. The strongest effects of radiation are seen at the cavity wall. Here, vaporization of the salt by the incident radiation causes some dispersion in the air shock and a reduction in the peak amplitude at the air-cavity interface. Within the salt, however, this effect is much reduced and the pressure and impulse time histories computed with and without radiation at the 25 m range shown in Figures 13 and 14 are nearly identical, except for a time delay introduced by the dispersion of the shock front in the radiation case.

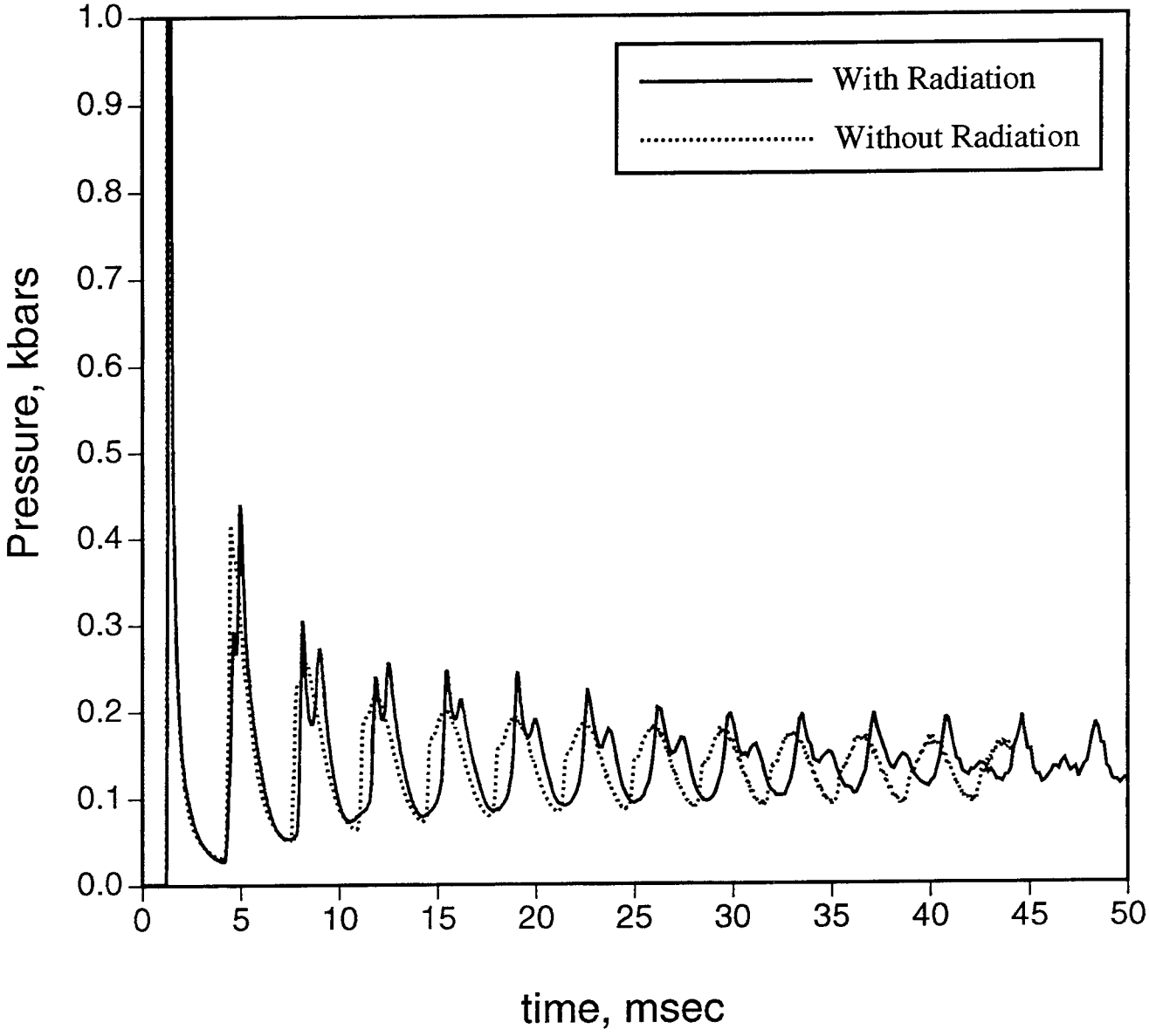

Figure 11. Comparison of pressure time histories at the cavity wall computed with and without radiation effects for a 380 ton nuclear explosion in a 17m radius, air-filled cavity in salt.

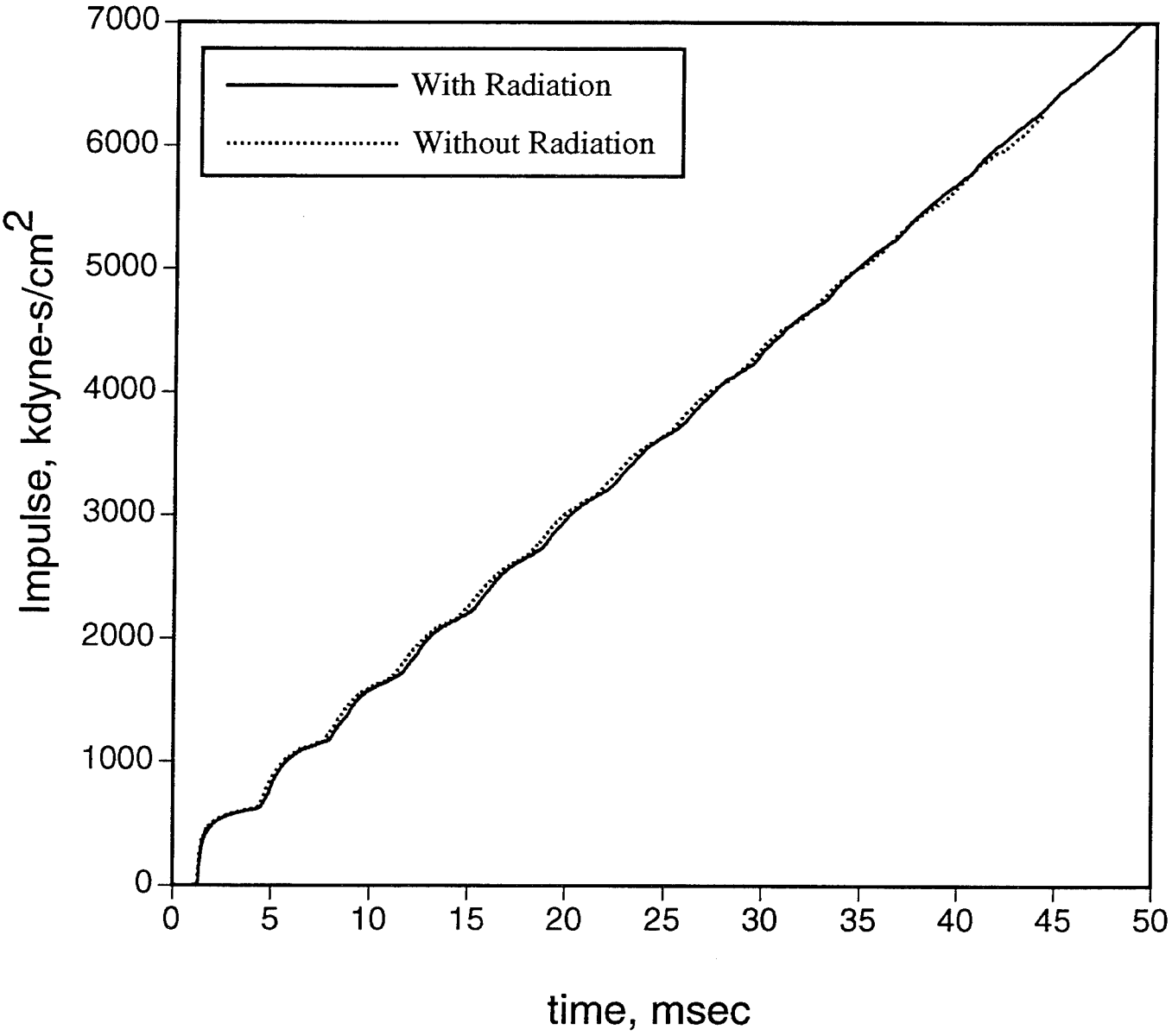

Figure 12. Comparison of impulse time histories at the cavity wall computed with and without radiation effects for a 380 ton nuclear explosion in a 17m radius, air-filled cavity in salt.

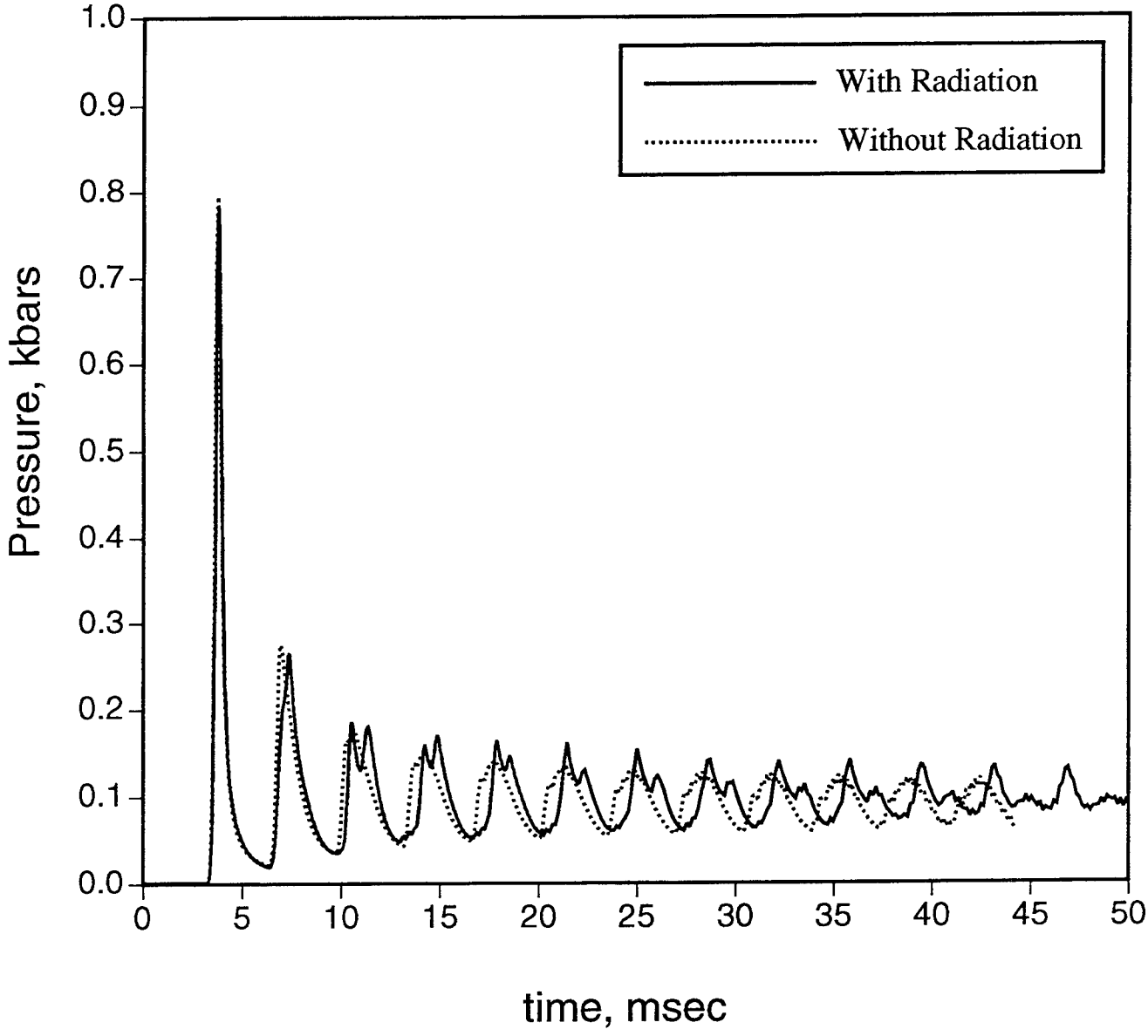

Figure 13. Comparison of pressure time histories at a range of 25m computed with and without radiation effects.

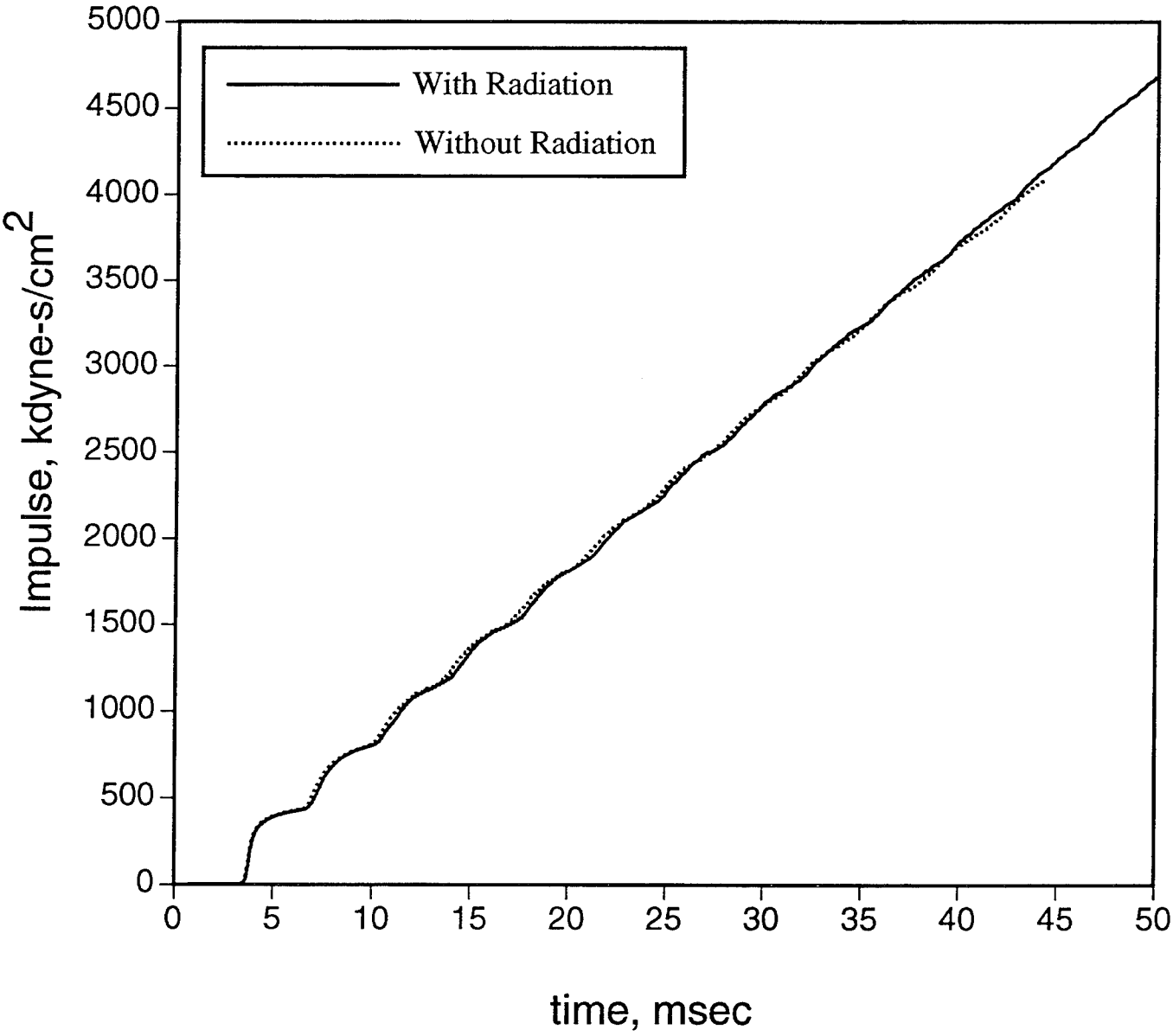

Figure 14. Comparison of impulse time histories at a range of 25m computed with and without radiation effects.

An additional calculation with radiation was performed to assess the effect of zone size on the computed motions. In this calculation, the first zone size was reduced by a factor of ten to 11 microns, again with a zoning ratio of 1.05. This was a very time consuming calculation which required more than a week of CPU time on an SGI Indigo computer to complete. The computed pressure and impulse time histories at a range of 25 m from this calculation are shown in Figures 15 and 16, respectively, where they are compared with the corresponding time histories from the much larger zone size calculations of Figures 13 and 14. It can be seen that these two sets of computed motions are essentially identical, confirming the adequacy of the larger zone sizes for these calculations.

In order to assess the effects of variations in assumptions about air opacity, three supplemental calculations were performed in which the air opacity was reduced by factors of 10, 100 and 1000, thereby allowing progressively more radiation to reach the cavity wall. The maximum reduction in opacity resulted in only a three percent decrease in the computed impulse within the salt. The timing was affected, especially at times less than 15 ms, due to the increase in material ablated from the cavity wall prior to shock arrival. The reflection time of the pressure waves was increased by 4-6 ms when the opacity was decreased by a factor of 1000, but decreases of factors of less than 100 were found to have little effect. Figures 17 and 18 show comparisons of the pressure and impulse time histories computed at a range of 25 m with air opacity reduction factors of 1, 10, 100 and 1000.

In summary, the results of the various simulations described above indicate that the effect of radiation on the transmitted pressure and impulse from a nuclear explosion in an air-filled cavity is small. That is, these results do not support the hypothesis that radiation has a significant influence on the decoupling effectiveness of air-filled cavities.

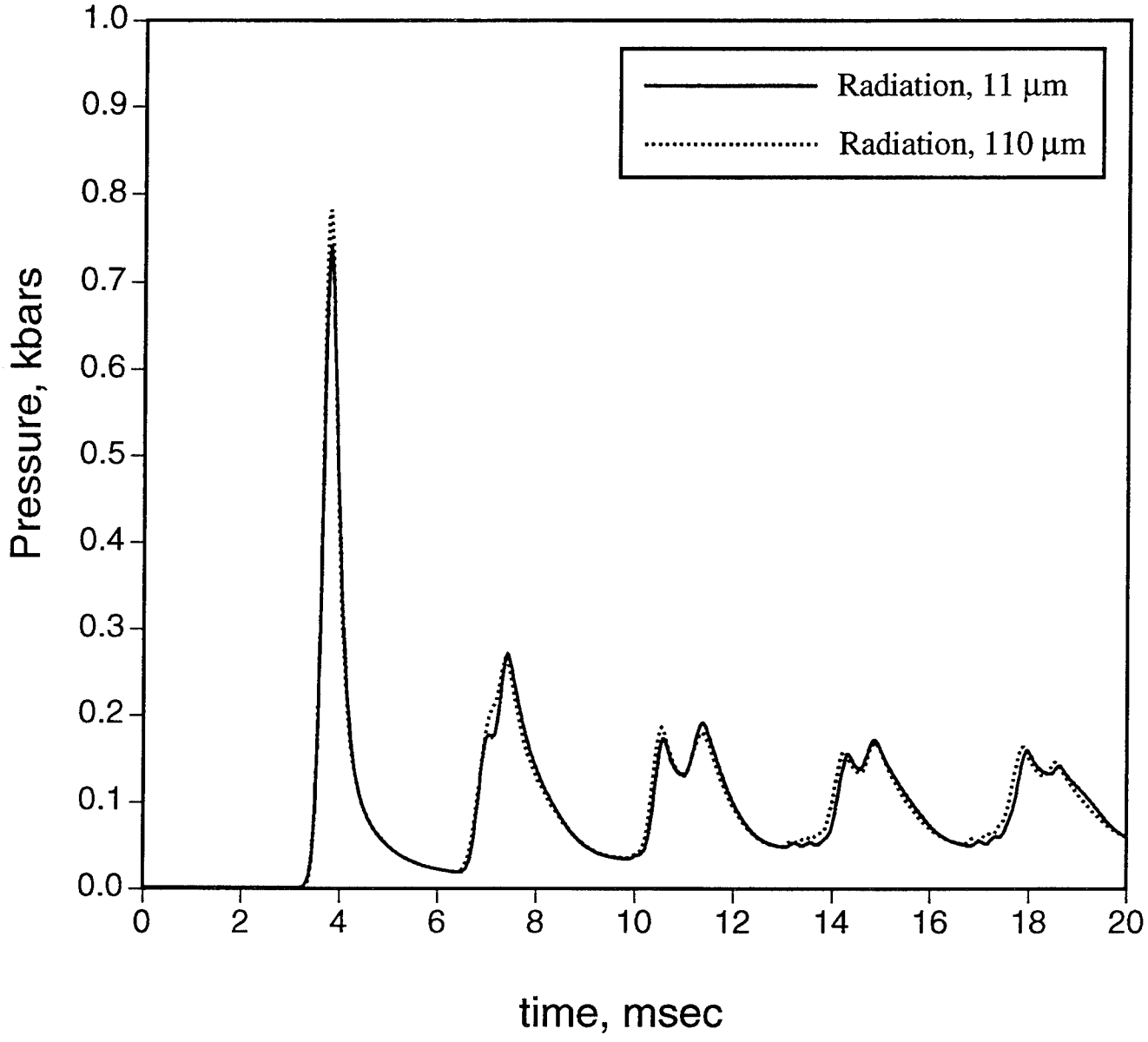

Figure 15. Comparison of pressure time histories at a range of 25m computed with radiation effects for initial zone sizes of 11 and 110 microns.

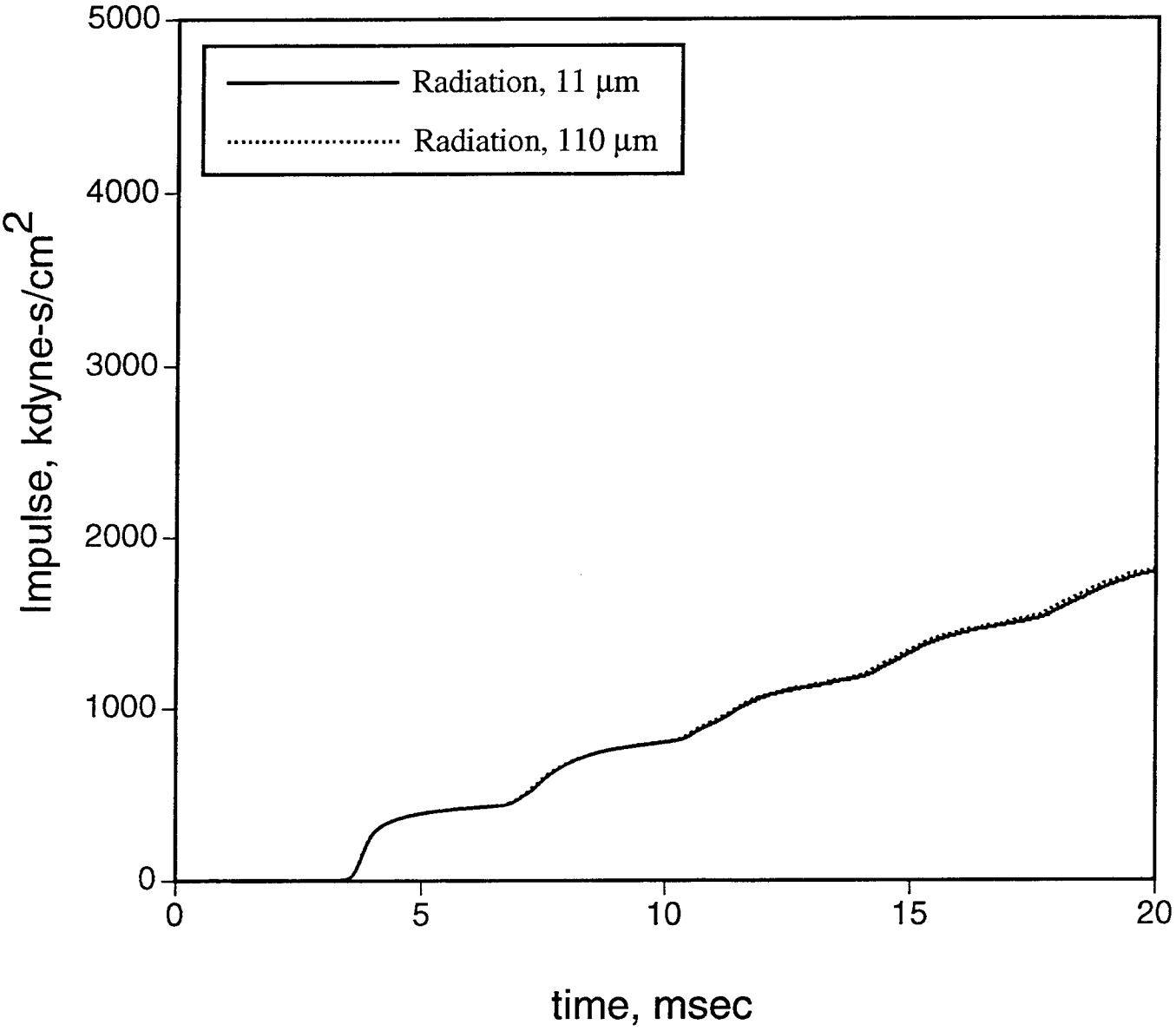

Figure 16. Comparison of impulse time histories at a range of 25m computed with radiation effects for initial zone sizes of 11 and 110 microns.

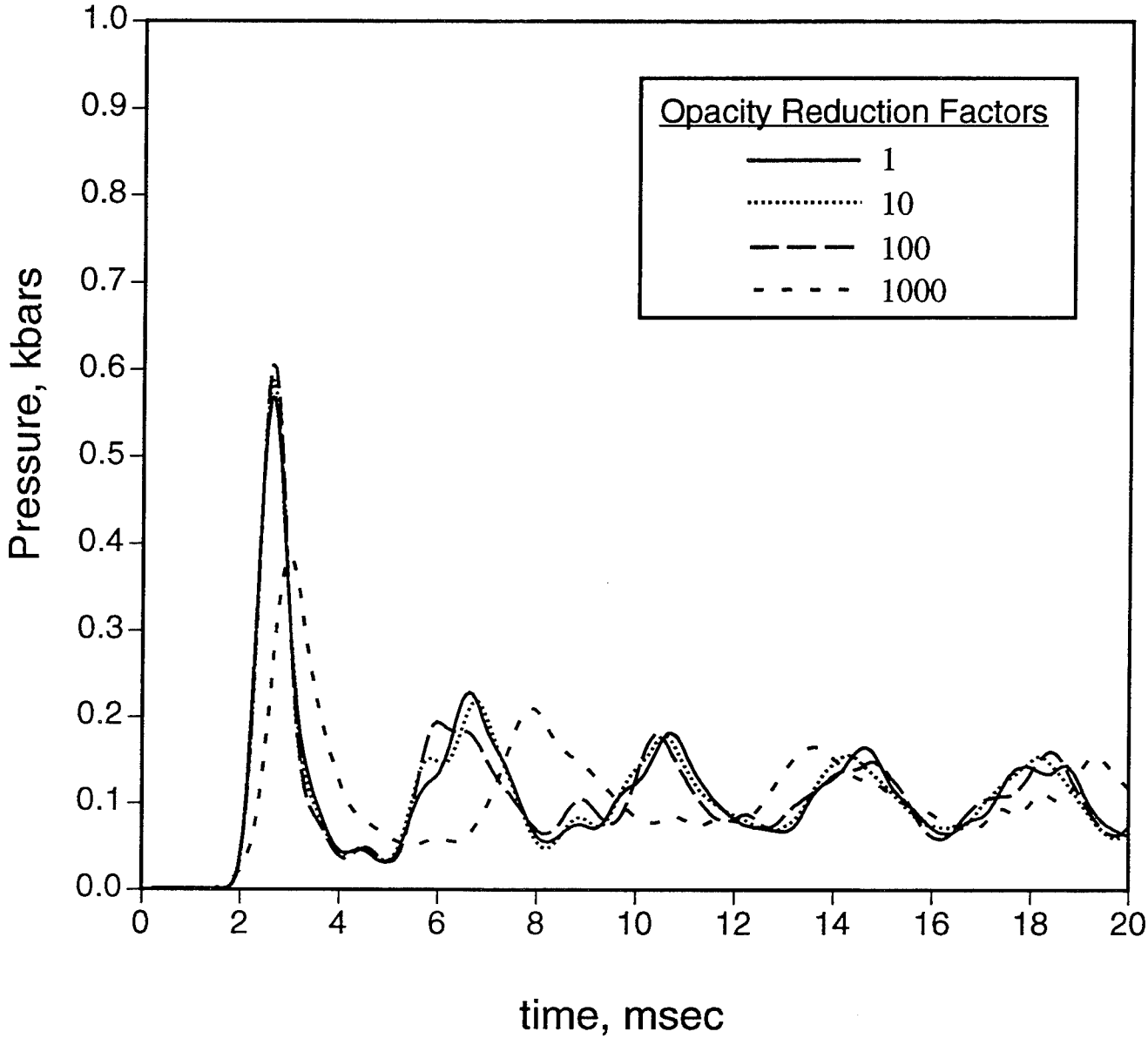

Figure 17. Comparison of pressure time histories at a range of 25m computed with radiation effects for air opacities reduced by factors of 1, 10, 100 and 1000 with respect to the nominal value.

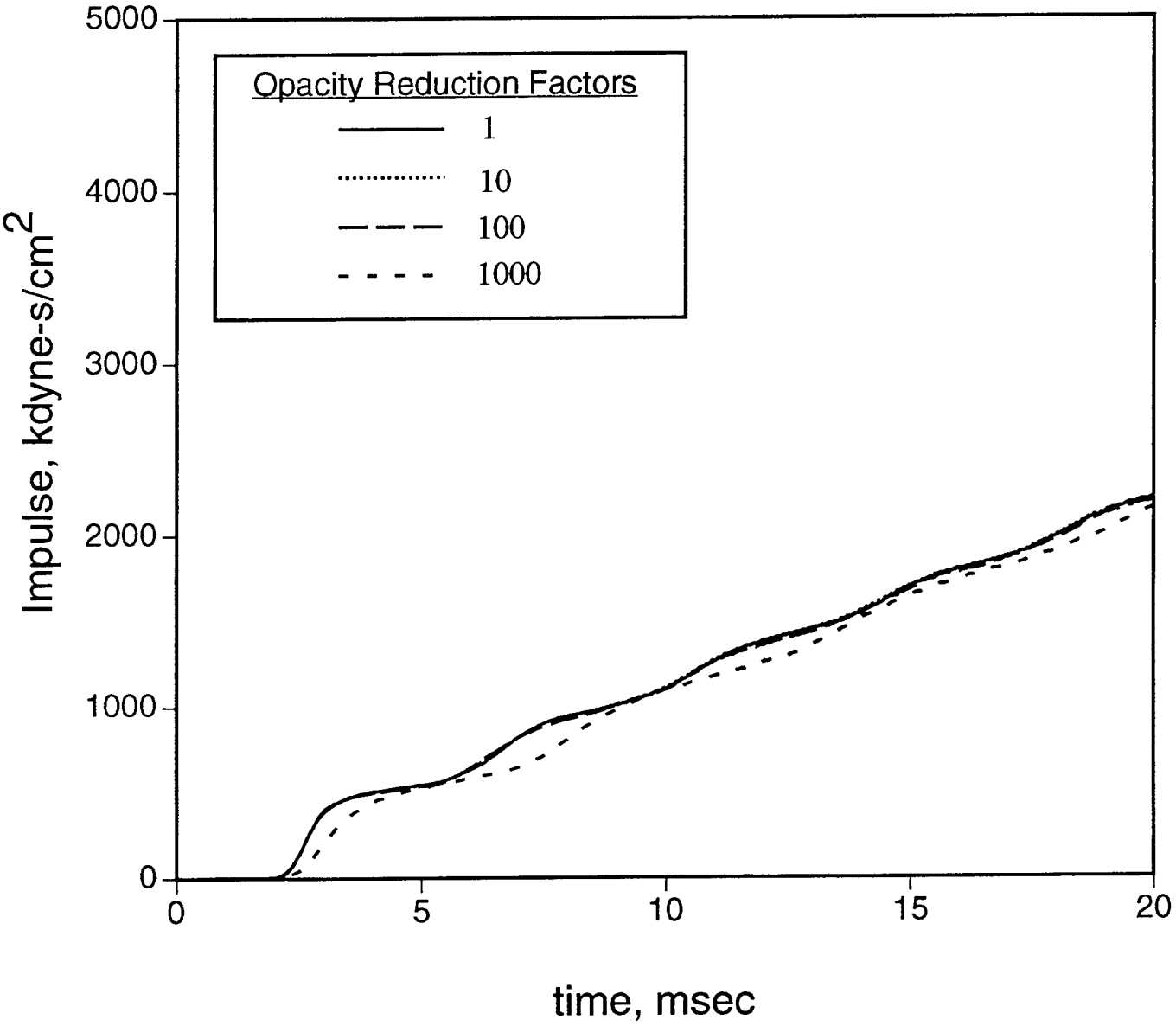

Figure 18. Comparison of impulse time histories at a range of 25m computed with radiation effects for air opacities reduced by factors of 1, 10, 100 and 1000 with respect to the nominal value.

4. AZGIR WATER-FILLED CAVITY EXPERIMENTS

The Russian nuclear test site at Azgir is situated in the northwest part of the Caspian Depression of the Russian Platform, near the border between the Astrakhan District and Kazakhstan. The Caspian Depression is characterized by thick sediments (up to 7 km) and intensive salt dome tectonics. The salt is generally covered by a 1-2 km thick layer of sediments, but the upper surfaces of the salt domes are encountered at depths of only 200-400 m in some locations, with occasional surface outcrops, such as that near the town of Azgir. One of these salt dome structures, known as the Great Azgir salt deposit, was used as a scientific test site to conduct 17 peaceful nuclear explosions (PNE) during the period from 1966 to 1979. This deposit consists of two domes, denoted the West and East Azgir salt domes, both of which were used in the testing program. The goals of this PNE test series conducted at Azgir were to address specific scientific problems and to develop new technologies for industrial applications of underground nuclear explosions.

The A2 emplacement hole at Azgir is located in the northern part of the West dome at 47.9086°N, 47.9119°E and penetrates to a depth of 600 m with a diameter of 0.63 m. The stratigraphic sequence at this location consists of a 240 m layer of sediments, overlying a 56 m thick anhydrite cap layer which, in turn, overlies the massive salt formation which extends to the bottom of the hole and beyond. The hole was cased to a depth of 300 m, or to just below the anhydrite/salt interface. The nominal elastic properties of the salt medium, determined from laboratory analysis of samples recovered from emplacement hole A-2 indicate a compressional wave velocity of about 4250 m/sec, a shear wave velocity of about 2400 m/sec and a density of about 2.2 gm/cm^3. These values are quite comparable to those reported for the Tatum salt dome in Mississippi where the U.S. nuclear tests SALMON and STERLING were conducted. In fact, comparisons of free-field seismic data recorded from SALMON and tamped Azgir explosions suggest that the

seismic source coupling is quite similar in these two salt domes (Murphy and Barker, 1994). These observations suggest that it should be possible to evaluate the seismic data recorded from the Azgir water-filled cavity tests using material models similar to those previously validated for the Tatum salt dome.

A tamped explosion with a yield of about 25 kt was conducted at a depth of 597.2 m in emplacement hole A2 on 7/01/68. This explosion produced a stable, roughly spherical cavity which subsequently filled with water which flowed in from the pierced water table above the cap rock. A post-test, downhole survey indicated that this cavity had a maximum horizontal radius of 32.5 m and a total volume of 101,000 m^3. This total volume is equal to that which would be associated with a purely spherical cavity with a radius of 28.9 m. Six nuclear explosions with different yields were detonated in this water-filled cavity in the period from 1975 to 1979. In each case, the emplacement hole was filled with water prior to the test and a special containment lock was established in the upper part of the hole to prevent water ejection. Slight variations of cavity shape and volume were observed after each explosion. For example, after the first 0.35 kt water-filled cavity explosion of 4/25/75, a volume increase of 3000 m^3, or about 3%, was measured. A detailed cavity survey was conducted following the fourth water-filled cavity test of 9/12/78 and the results are summarized in Figure 19. This figure indicates that the depth to the bottom of the cavity has decreased by about 3 m (from 595 to 592 m) due to accumulation of fragments of cables, casing and salt which have fallen into the cavity as a result of the repeated testing. However, the depth to the top of the cavity has also decreased by about 3 m (from 555 to 552 m) due to spallation of the cavity roof material, so the vertical extent of the cavity remains virtually unchanged. Thus, although the repeated testing damaged the cavity walls to some extent in this case, the Russian experience at Azgir indicates that it is feasible to conduct multiple nuclear tests in a sufficiently large cavity in such a manner that cavity collapse or significant venting of material will not occur.

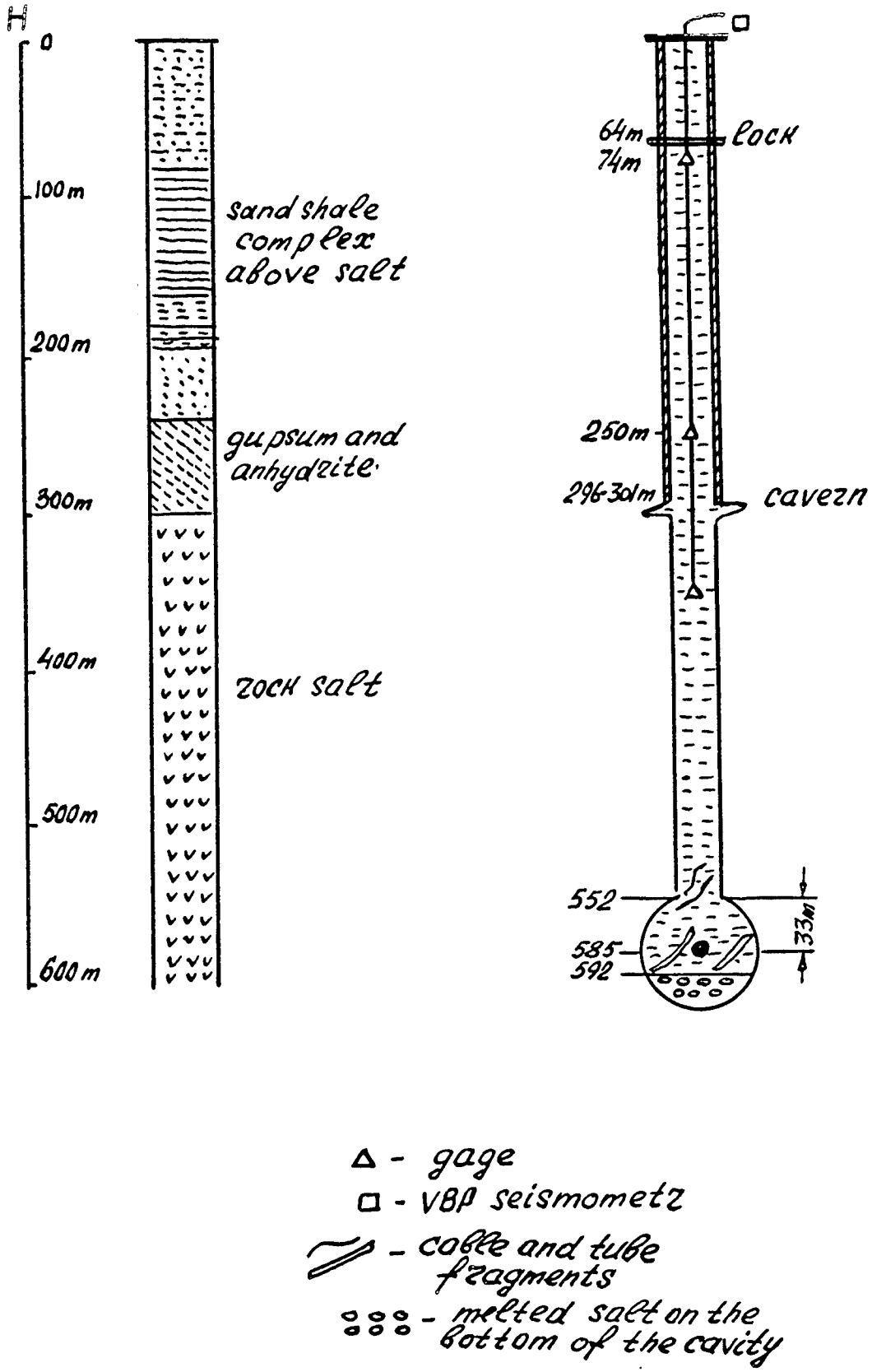

Figure 19. Schematic drawing illustrating the cavity condition following the fourth Soviet nuclear test in the water-filled cavity at Azgir. The section at the left shows the subsurface geologic profile down to shot depth at this site.

The source parameters of the seven nuclear explosions conducted in emplacement hole A2 at Azgir are listed in Table 1, where it can be seen that the yields of the water-filled cavity explosions varied over a factor of 50, ranging from 0.01 to 0.50 kt. Now a 28.9 m radius, air-filled cavity at a depth of 585 m in salt would be expected to decouple a 1.3 kt explosion to the same degree as that achieved for the U.S. STERLING explosion. It follows that if this cavity had been air-filled, all of the A2 cavity tests would have been fully decoupled and the associated seismic signals would have been well below the teleseismic detection threshold. In fact, however, the two largest of these cavity explosions (i.e. A2-2 and A2-7) were detected at teleseismic distances and have been assigned m_b values in the 4.0 to 4.5 range. Since a fully tamped 1 kt explosion in salt at Azgir corresponds to an m_b value of 4.5 or less (Murphy and Barker, 1994), it follows that these cavity tests were not decoupled and, in fact, seem to show enhanced coupling over some frequency bands, more consistent with what would be expected for explosions in water (Evernden, 1970). Nevertheless, the seismic data recorded from these cavity tests can provide important information relevant to the assessment of cavity decoupling in salt in that they represent a well-controlled series of tests in a single cavity in which the yields varied by a factor of 50. A systematic analysis of these data should provide important new constraints on the dynamic response characteristics of salt under explosive loading.

Seismic data from this series of explosions in Azgir emplacement hole A2 were recorded at 28 stations located in the near-regional distance range extending from about 1 to 175 km. Both vertical and horizontal radial component data were recorded at stations located within 20 km of ground zero and full, three-component data sets were recorded at the more distant stations. Photographic recordings from the tamped explosion A2 and the first four of the water-filled cavity tests (i.e., A2-2, A2-3, A2-4, A2-5) have now been collected and carefully digitized at IDG using standardized procedures described by Kitov *et al.* (1994). Most of these data were digitized at sampling rates of 200 samples/second or higher, which provides more than adequate resolution of the highest frequency components which

Table 1

Source Parameters For Azgir Water-Filled Cavity Tests

Emplacement Coordinates: 47.9086N, 47.9119E

Event	Date	Origin Time, UT	Depth, m	Yield, kt*
A2	7-01-68	04 02	597.2	25
A2-2	4-25-75	05 00	582	0.35
A2-3	10-14-77	06 59 59.100	587	0.10
A2-4	10-30-77	06 59.59.069	586.2	0.01
A2-5	9-12-78	04 59 58.494	585	0.08
A2-6	11-30-78	04 59 58.929	586	0.06
A2-7	1-10-79	08 00	590	0.50

*Russian Ministry of Defence (personal communication, Ralph Alewine, 1994)

can be reliably recovered from this recording medium. At a number of stations, data were recorded from most or all of these tests on a common instrument, thereby providing a basis for direct comparisons in which the propagation paths are held constant. Samples of the vertical component data recorded at four stations in the distance range extending from 1.17 to 75 km are presented in Figures 20-23, where the initial P wave arrivals are shown plotted at a common time scale. It can be seen from these figures that the large differences in dominant frequency content between the tamped and cavity explosion seismic sources are quite evident at the closer stations (i.e., Figures 20-22), where the impulse responses of the propagation paths appear to be relatively simple. In fact, at the two closest stations at 1.17 and 1.71 km, consistent source differences can be detected among the signals produced by the various water-filled cavity tests. Thus, for example, it appears that the seismic signatures of A2-4 explosion are indicative of a longer duration, more reverberant source than those of the other three cavity tests.

As is illustrated in Figure 23, the situation is more complex at greater distances where the signals are significantly affected by frequency dependent attenuation along the propagation paths. Thus, at this station at 75 km distance, the frequency contents of the initial P wave arrivals from the tamped and cavity tests appear to be quite comparable, although the following P coda arrivals on the recordings from the cavity tests continue to show enhanced high frequency content. These differences are illustrated more clearly in Figure 24, which shows a comparison of longer time segments of these vertical component recordings at the 75 km station. The short vertical arrows plotted above these traces at about 11 seconds after first motion denote the approximate expected arrival time for direct S at this distance. It can be seen that this S arrival appears to be more prominent on the recordings from the water-filled cavity tests than on the recording from the tamped explosion. This difference is also apparent on the corresponding horizontal radial component recordings at this station which are shown in Figure 25. This apparent difference in S/P excitation efficiency is somewhat surprising in that these water-filled cavity explosions might be expected to

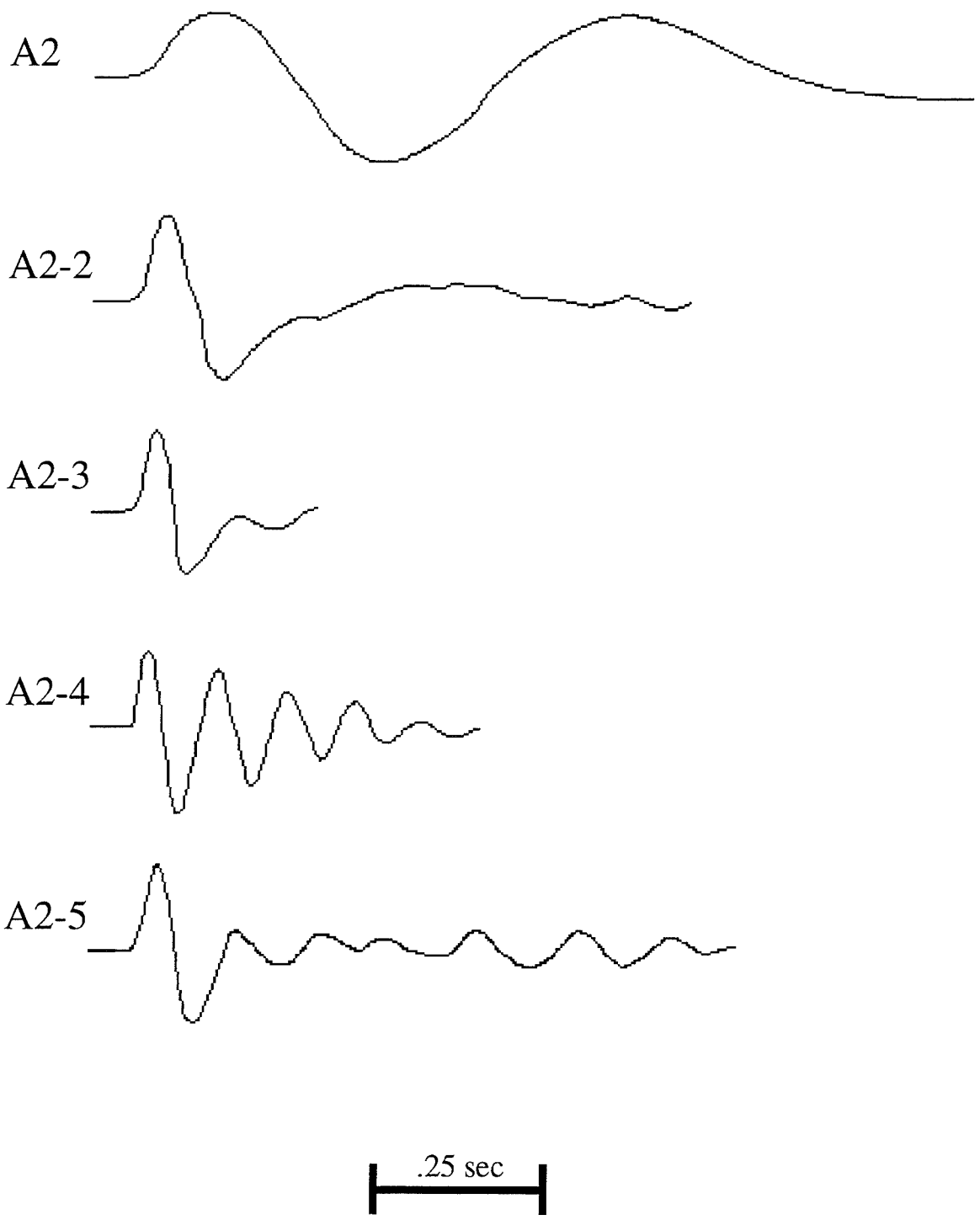

Figure 20. Comparison of vertical component seismic data recorded from the Azgir tamped and water-filled cavity explosions at a range of 1.17 km.

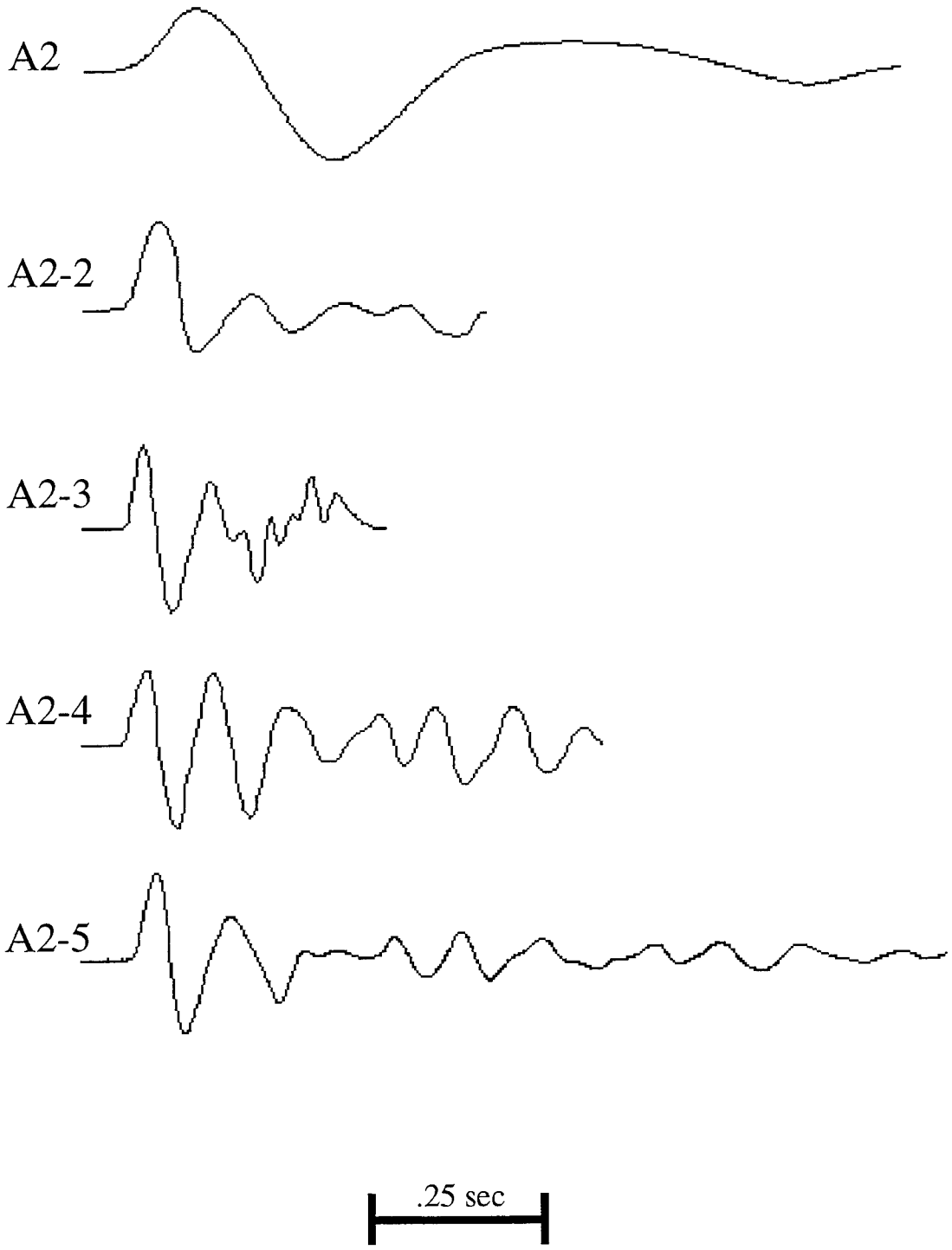

Figure 21. Comparison of vertical component seismic data recorded from the Azgir tamped and water-filled cavity explosions at a range of 1.71 km.

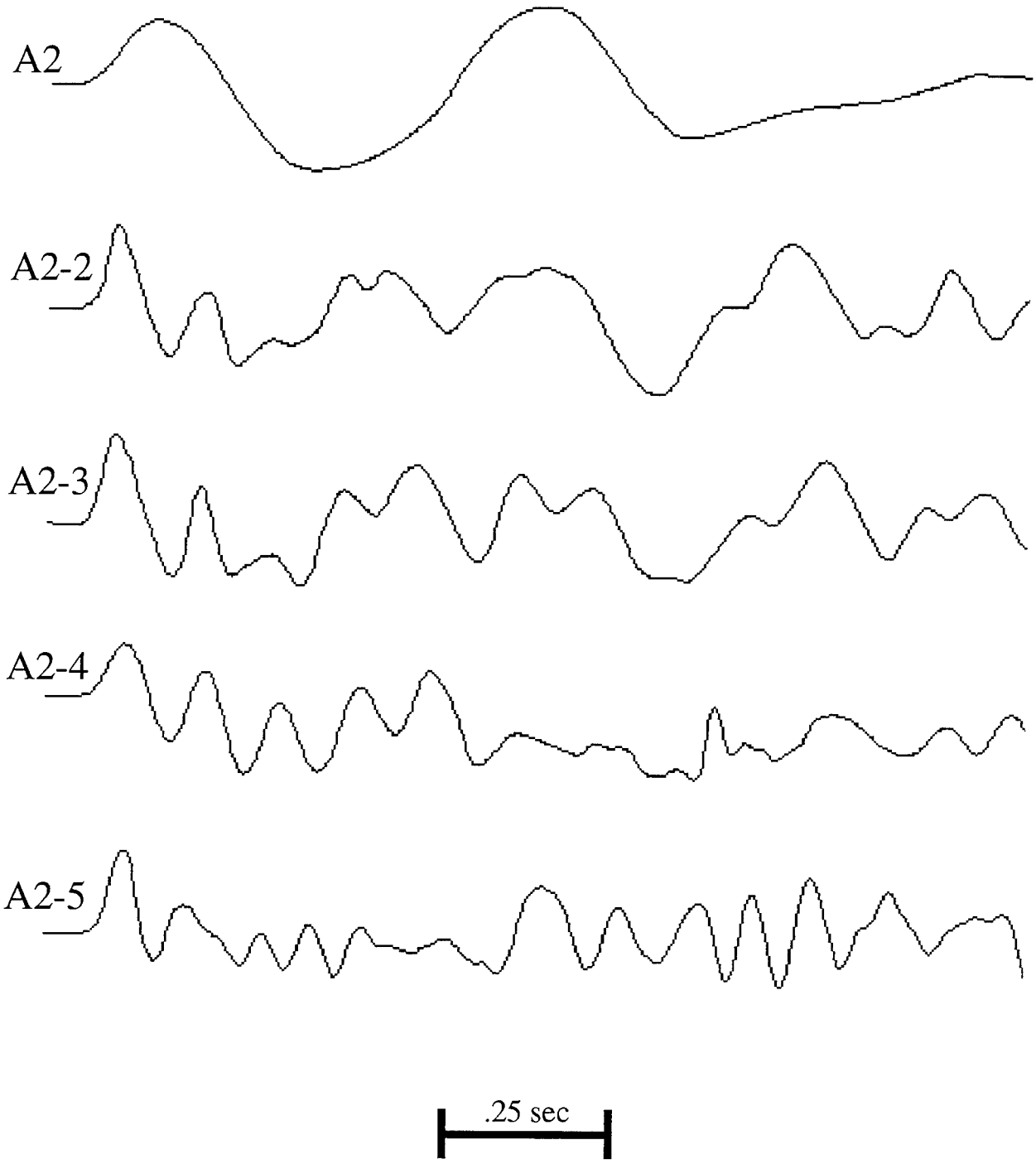

Figure 22. Comparison of vertical component seismic data recorded from the Azgir tamped and water-filled cavity explosions at a range of 7.8 km.

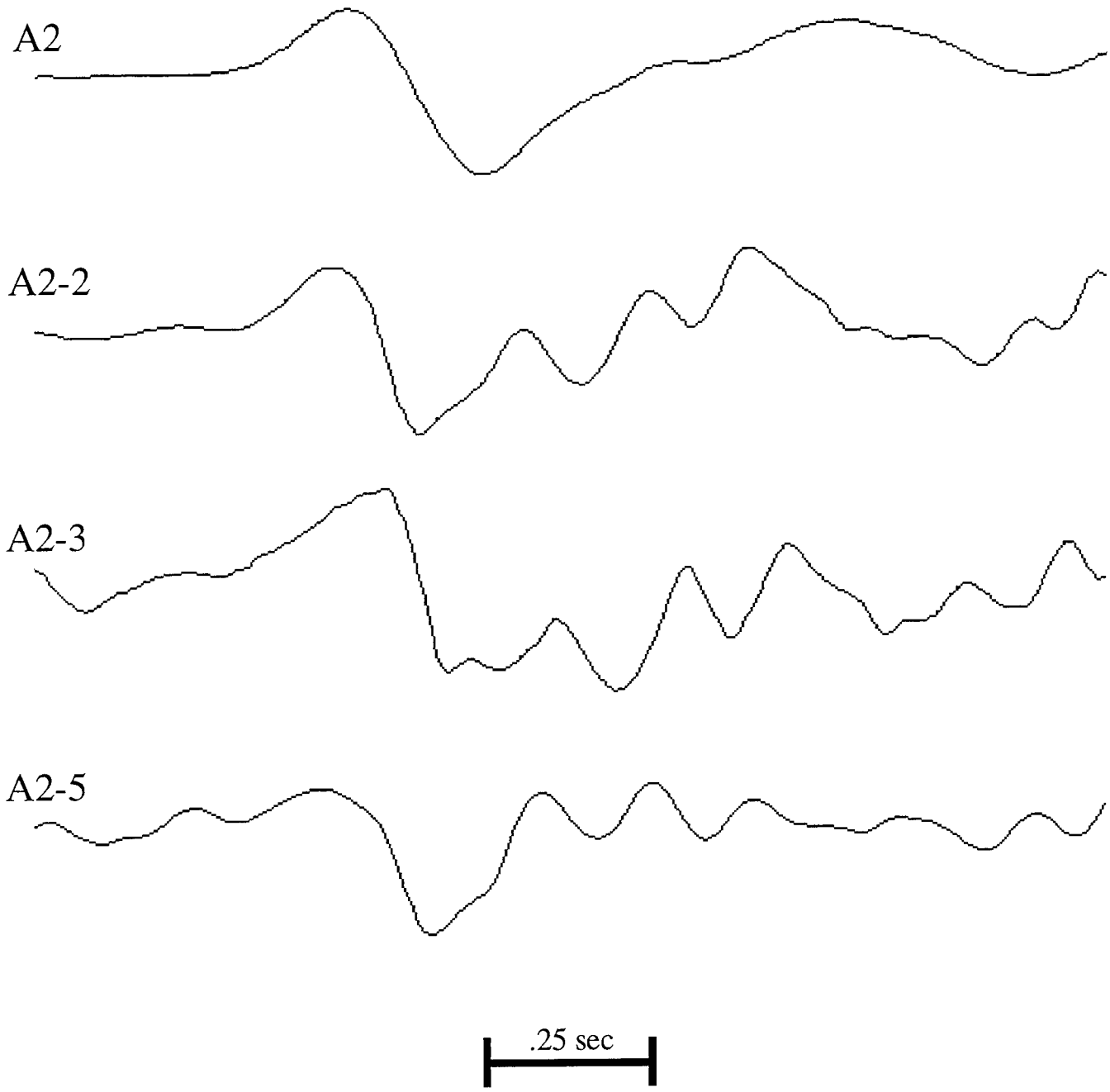

Figure 23. Comparison of vertical component seismic data recorded from the Azgir tamped and water-filled cavity explosions at a range of 75 km.

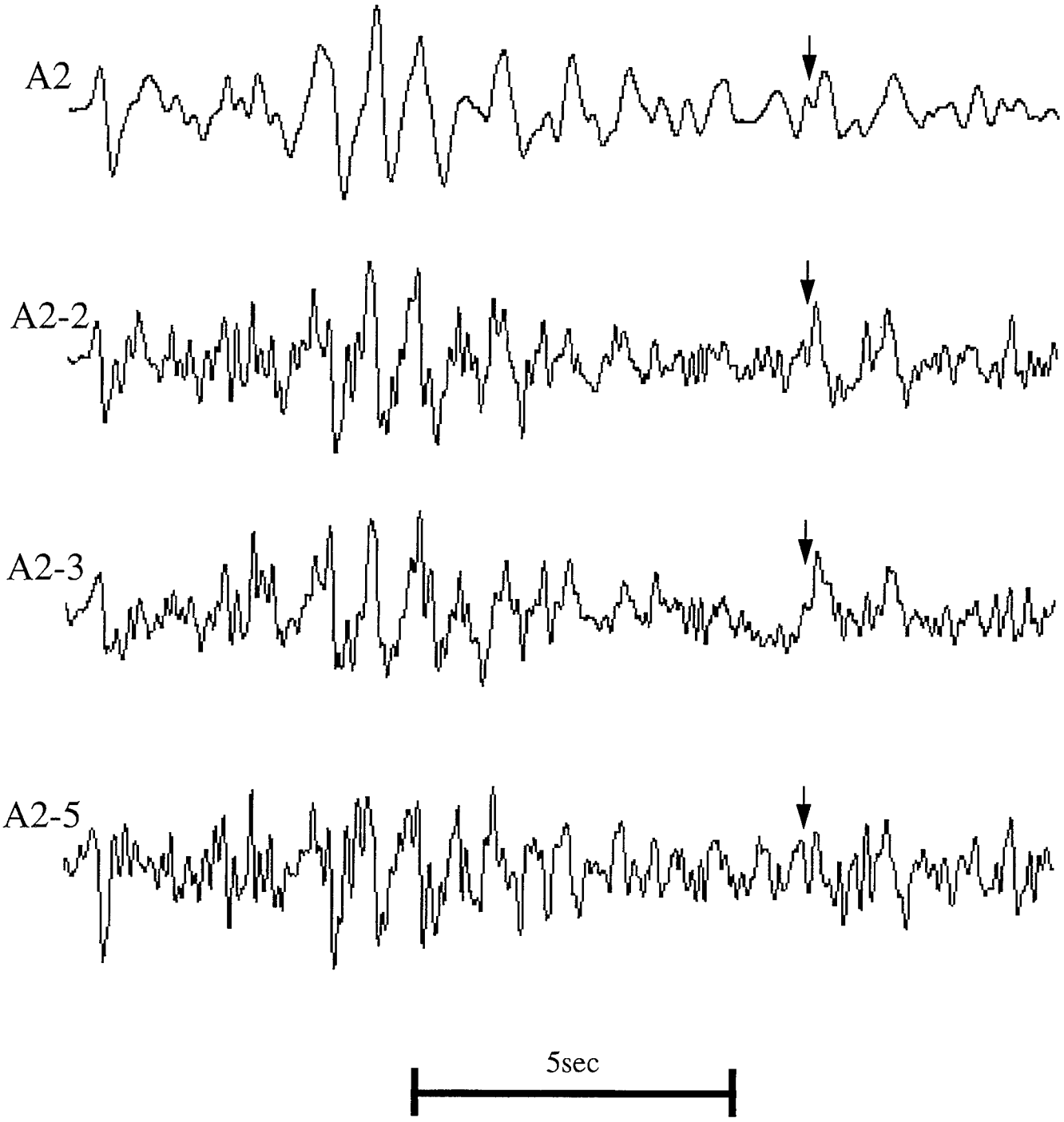

Figure 24. Comparison of P and S wave vertical component data recorded from the Azgir tamped and water-filled cavity explosions at a range of 75 km. Vertical arrows denote the approximate onset time of the direct S arrival.

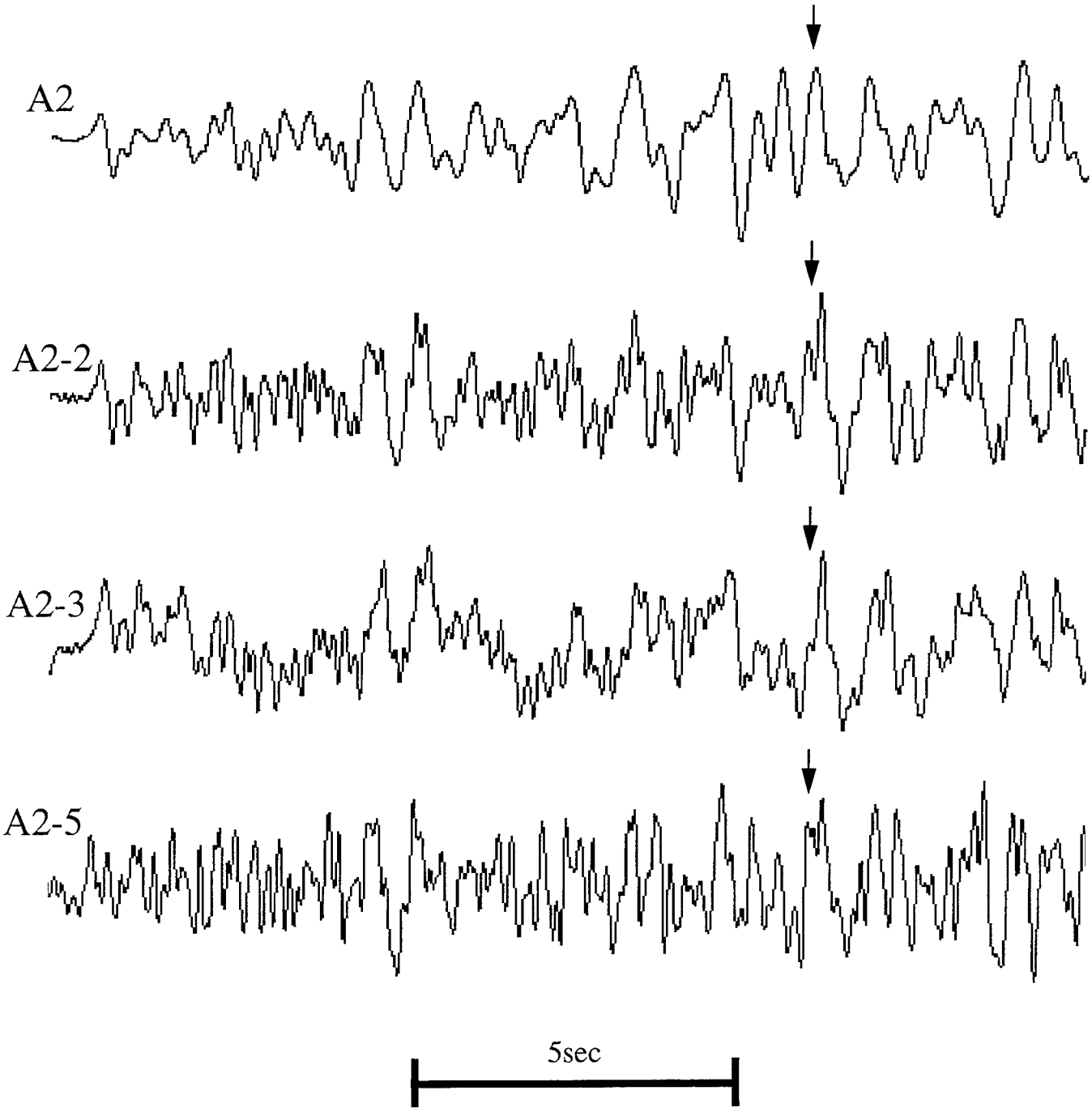

Figure 25. Comparison of P and S wave horizontal radial component data recorded from the Azgir tamped and water-filled cavity explosions at a range of 75 km. Vertical arrows denote the approximate onset time of the direct S arrival.

be more nearly spherically symmetric than the tamped test at the same location. However, more careful frequency dependent analyses will be required before any definitive conclusions can be drawn regarding the significance of this observation.

Quantitative analyses of the Azgir water-filled cavity tests are still in their initial stages, but we have recently completed several preliminary theoretical simulations of the seismic source functions corresponding to nuclear explosions of different yields conducted in 32 m radius water-filled, spherical cavities in salt. Two different salt equations of state, denoted "Laboratory salt" and "Rimer-Cherry salt," were used in these nonlinear, finite difference simulations of the water-filled cavity explosions (Stevens *et al.*, 1991). These generally encompass the rather broad range in seismic source coupling characteristics which have been proposed for this medium by different investigators over the years. The theoretical source spectral ratios computed for the different water-filled cavity tests with respect to fully tamped explosions of the same yields in Laboratory and Rimer-Cherry salt models are shown in Figures 26 and 27, respectively. It can be seen from these figures that both sets of calculations predict low frequency source spectral ratios of about unity, consistent with the observed teleseismic m_b values for these explosions which were referenced above. Moreover, both show pronounced resonance peaks in the 10 to 20 Hz band which appear to be associated with the dynamic response of the water in the cavity to the explosive loadings. However, on a more detailed level, a comparison of the spectral ratios of Figures 26 and 27 reveals significant differences in absolute amplitude levels and in the computed yield dependence over this range. It follows that a careful comparison with the observed data from these explosions should provide valuable constraints on the appropriate salt equation of state to be used in theoretical simulations of various cavity decoupling evasion scenarios.

The analyses of the corresponding observed data is also in progress and Figure 28 shows a preliminary comparison of the theoretical and observed source spectral ratios corresponding to the A2-3 0.1 kt water-filled

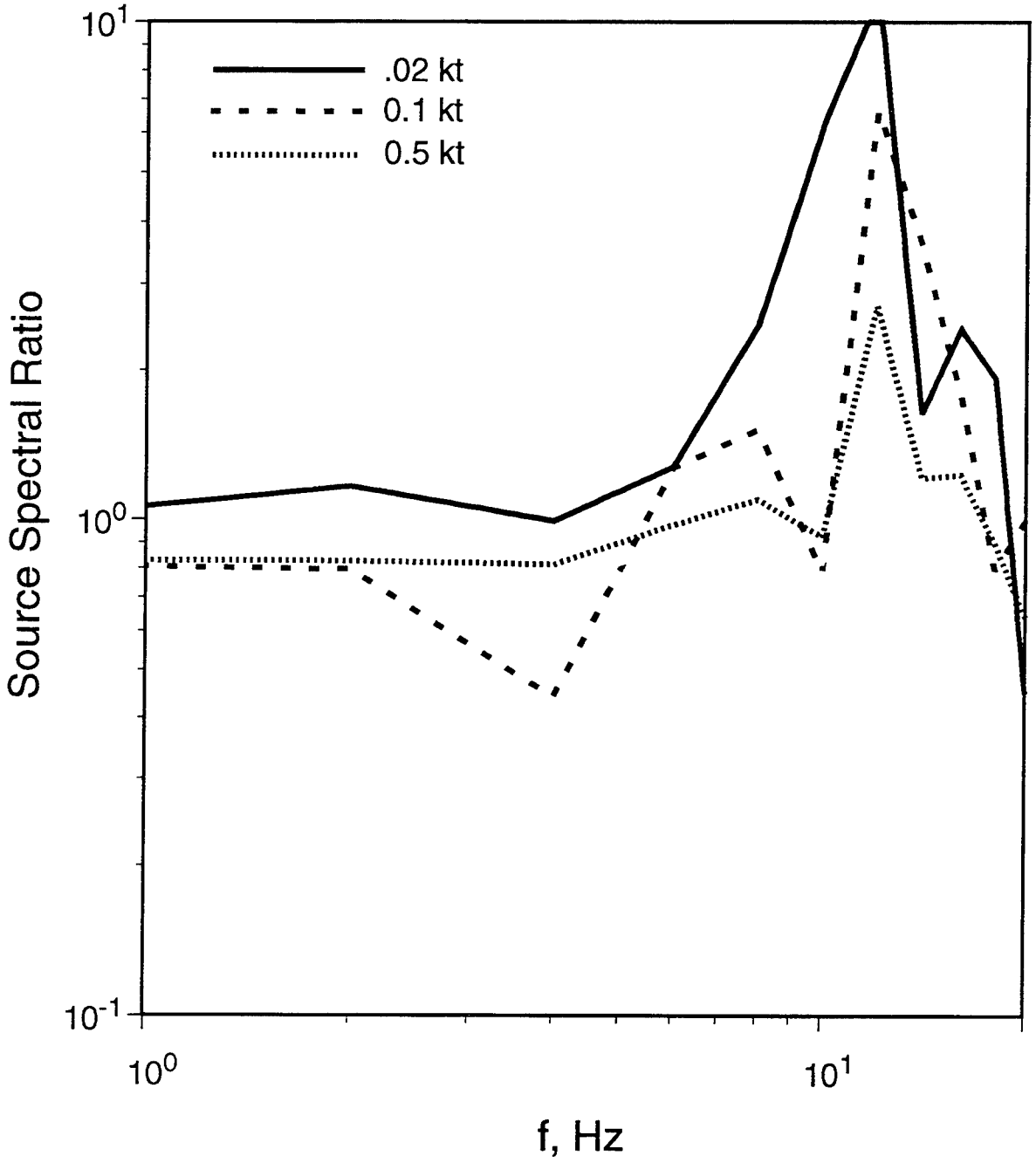

Figure 26. Comparison of theoretical source spectral ratios (cavity/tamped) for explosions of different yields in a 32m radius water-filled cavity in salt; Laboratory salt model.

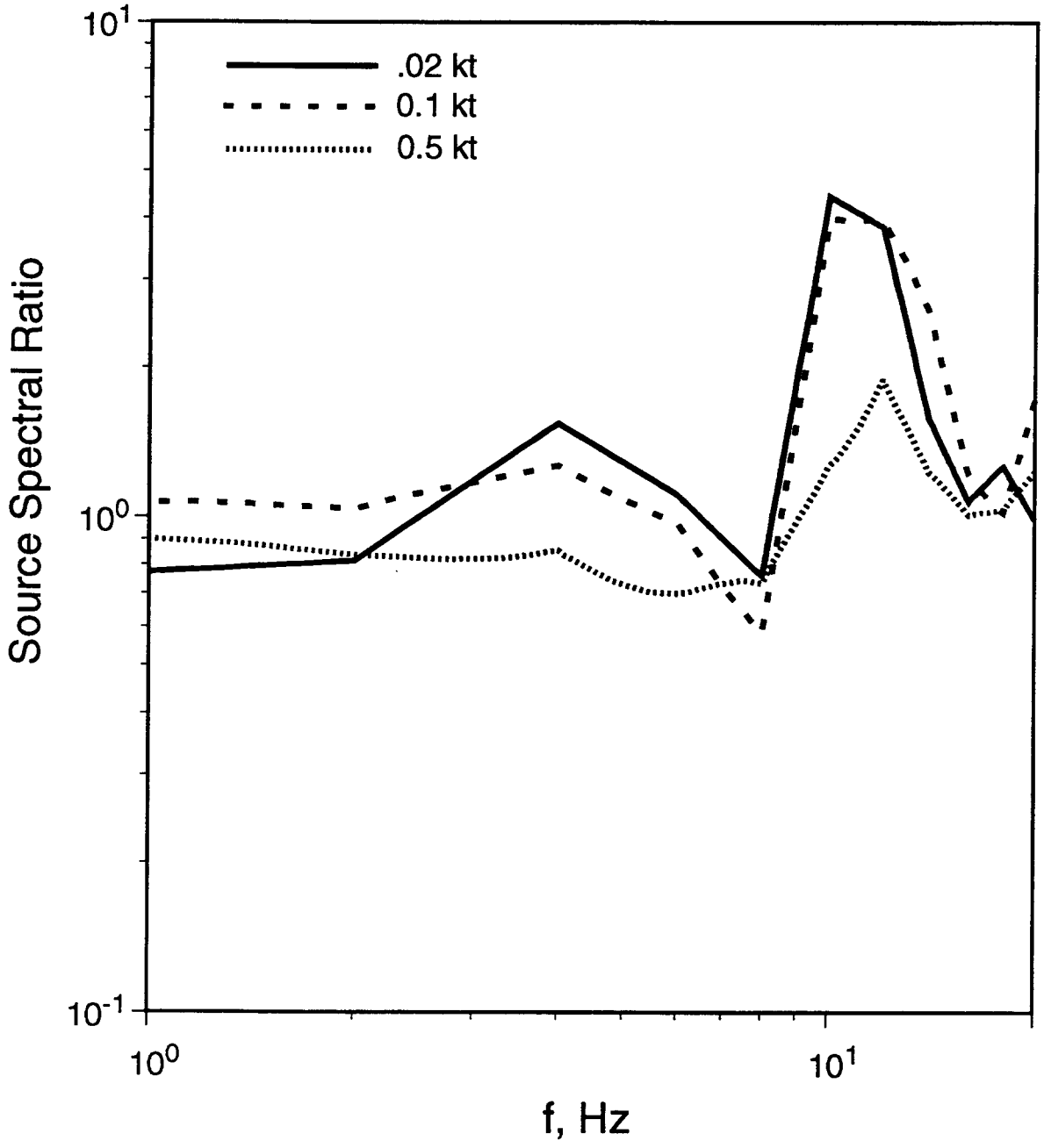

Figure 27. Comparison of theoretical source spectral ratios (cavity/tamped) for explosions of different yields in a 32m radius water-filled cavity in salt; Rimer-Cherry salt model.

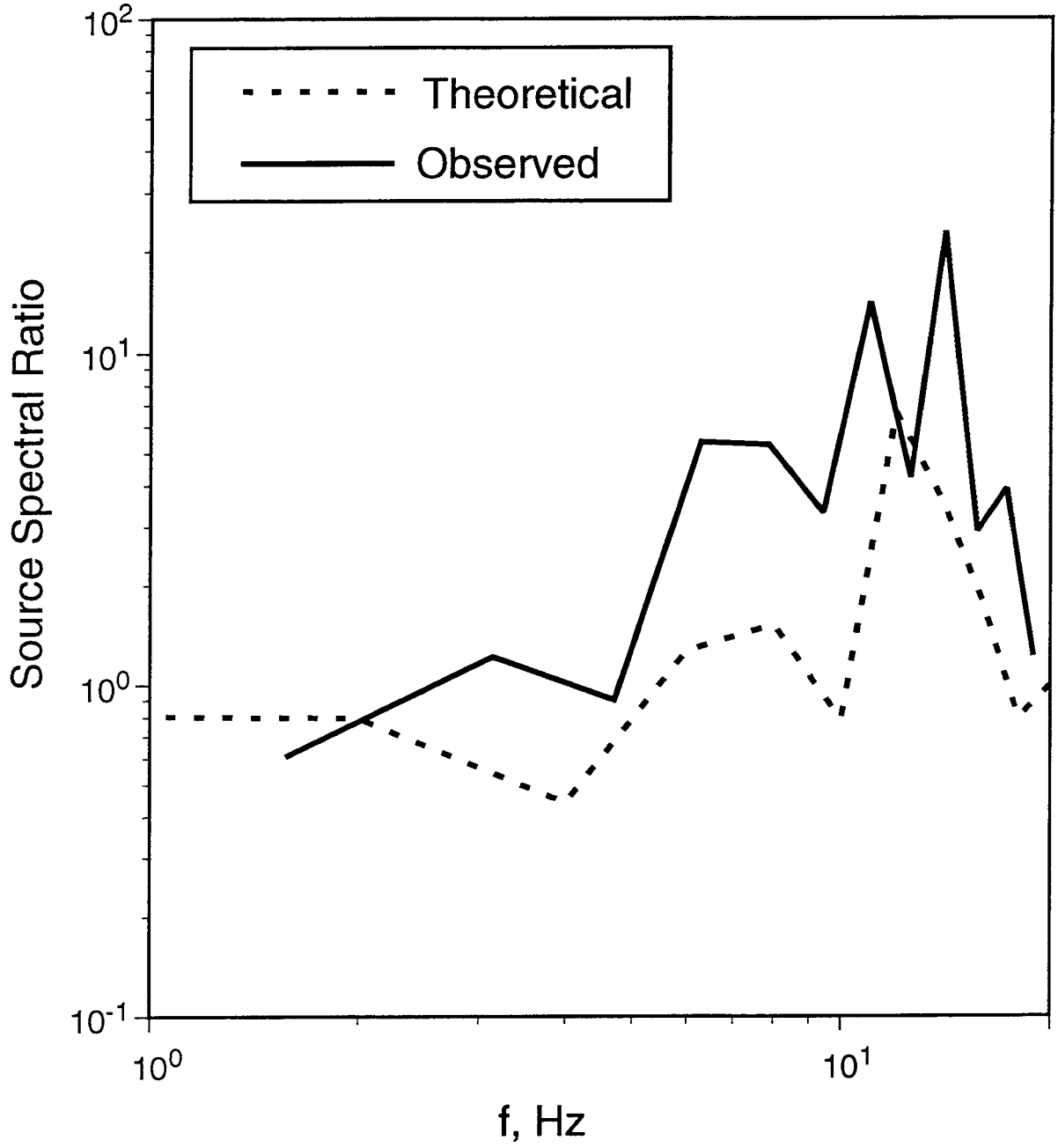

Figure 28. Comparison of theoretical and observed seismic source spectral ratios (cavity/tamped) for a 0.1kt nuclear explosion in a 32m radius water-filled cavity in salt.

cavity test. In this case, the theoretical ratio corresponds to the Laboratory salt result of Figure 26 and the observed ratio was determined from the 1.17 km and 1.71 km recordings of the A2 and A2-3 explosions shown previously in Figures 20 and 21, with cube root yield scaling of the A2 seismic source estimate to a yield of 0.1 kt. It can be seen that the result of the nonlinear theoretical simulation is in qualitative agreement with the observed data in this case, with both showing a ratio near unity at low frequencies and pronounced resonance peaks in the 10-15 Hz frequency band. However, much additional data will have to be processed and analyzed before any quantitative conclusions can be drawn regarding the fidelity of these theoretical simulation models.

5. SUMMARY AND CONCLUSIONS

This report has provided a summary of the initial results of an on-going joint research program in which S-CUBED scientists are working with scientists from the Russian Institute for Dynamics of the Geospheres (IDG) in an attempt to develop a better understanding of the effects of cavity decoupling on the seismic signals produced by underground nuclear explosions. These studies have included analyses of seismic data recorded from an extensive series of Russian HE cavity decoupling tests, a theoretical evaluation of the importance of radiation diffusion effects on nuclear cavity decoupling efficiency and an analysis of data from six Russian nuclear tests conducted in a water-filled cavity at the Azgir test site. The current status of these various investigations are briefly summarized in the following paragraphs.

5.1 Kirghizia HE Decoupling Tests

- During the summer of 1960 the Russians carried out an HE cavity decoupling test series in limestone at a site in Kirghizia. These tests were comparable to, and in some ways more extensive than, the corresponding COWBOY HE decoupling test series which was conducted in salt in the U.S. at about the same time. In particular, the Kirghizia series included tests designed to evaluate the effects of cavity shape and charge emplacement geometry on decoupling effectiveness.

- Evaluations of the peak amplitude data recorded from the Kirghizia tests suggest that decoupling effectiveness in limestone is roughly independent of cavity radius for explosions in spherical cavities having scaled radii greater than that of STERLING. These data also suggest that decoupling effectiveness is approximately independent of shape for roughly prolate spheroidal cavities with

aspect ratios of 3 to 1 or less. Both these results are consistent with our previously reported theoretical simulation results (Stevens *et al.*, 1991a,b).

- The results of a preliminary spectral analysis of selected Kirghizia seismic waveform data are consistent with a maximum low frequency decoupling factor of about 50 for fully decoupled HE explosions in spherical cavities in limestone.

5.2 Evaluation of the Effect of Nuclear Radiation on Seismic Decoupling

- A series of theoretical simulations of nuclear cavity decoupling has been carried out to further evaluate the suggestion of Glenn and Goldstein (1994) that radiation can have a significant influence on the decoupling effectiveness of air-filled cavities in salt.

- Coupled radiation/hydrodynamic calculations were performed for a 380 ton nuclear explosion in a 17 m radius, air-filled cavity in salt (i.e., STERLING equivalent) using the Lagrangian finite difference code ZOOS. These theoretical simulations were performed with and without radiation, and employed a wide range of different air opacities.

- Comparisons of our computed pressure and impulse time histories with and without radiation at the cavity wall and at various ranges in the surrounding salt indicate that the effects of radiation are very small in this case. We conclude that radiation does not have a significant influence on the decoupling effectiveness of air-filled cavities.

5.3 Azgir Water-Filled Cavity Experiments

- During the period 1975-1979, the Russians conducted six small nuclear tests in the 32 m radius, water-filled cavity produced by a previous tamped explosion in salt at the Azgir test site. These tests extended over a range of a factor of 50 in yield (i.e., 0.01 to 0.50 kt) and have provided a unique set of seismic data which are being analyzed to further investigate the seismic source characteristics of explosions in salt.

- As part of the testing procedure, the cavity condition was resurveyed after each of these six explosions. These surveys revealed that, although the repeated testing damaged the cavity walls to some extent, it is feasible to conduct multiple nuclear tests in a sufficiently large cavity in such a manner that cavity collapse or significant venting of radioactive material will not occur.

- Seismic data recorded at both near-regional and teleseismic distances from the nuclear explosions in the water-filled cavity indicate that these tests were not decoupled in the manner which would be expected for comparable explosions in an air-filled cavity. Preliminary empirical and theoretical evaluation of the seismic source characteristics of these tests reveal low frequency source coupling factors comparable to those of tamped explosions of the same yield and strong resonance peaks in the 10-15 Hz band which appear to be associated with the dynamic response of the water in the cavity to the explosive loadings.

References

Adushkin, V. V., D. D. Sultanov, I. O. Kitov and O. P. Kuznetsov (1992), "Overview of the Experimental Data and Theoretical Simulations of Underground Nuclear Explosions Decoupled by Large Air Filled Cavities," *Rep. Russian Acad. Sci.*, 327 (1).

Evernden, J. F. (1970), "Magnitude versus Yield of Explosions," *Journal of Geophysical Research, Vol. 75*, No. 5, p. 1028.

Glenn, L. A. and P. Goldstein (1994), "Seismic Decoupling With Chemical and Nuclear Explosions in Salt," *Journal of Geophysical Research, Vol. 99*, No. B6, p. 11,723.

Kitov, I. O., V. V. Adushkin, V. N. Kostuchenko, O. P. Kuznetsov and D. D. Sultanov (1994), "Procedures for Photographic Paper Record Digitizing," Scientific Report Number 1 on Contract 911412, August.

Latter, A. L. (1959), "Verbatim Record of Technical Working Group 2, Conference on the Discontinuance of Nuclear Weapons Tests," GEN/DNT/TWG, 2/PV, December.

Murphy, J. R., J. L. Stevens and N. Rimer (1988), "High Frequency Seismic Source Characteristics of Cavity Decoupled Underground Nuclear Explosions," S-CUBED Technical Report SSS-TR-88-9595 (AFGL-TR-88-0130), ADA198121.

Murphy, J. R. and B. W. Barker (1994), "Seismic Identification Analyses of Cavity Decoupled Nuclear and Chemical Explosions," S-CUBED Technical Report SSS-TR-94-14399 (PL-TR-94-2036). ADA280947

S-CUBED (1969), The VERA System of Radiation-Hydrodynamics Codes," S-CUBED Radiation Group Report 3SCR-67-1 to DASA, DASA Report 2258-I, February.

Stevens, J. L., J. R. Murphy and N. Rimer (1991a), "Seismic Source Characteristics of Cavity Decoupled Explosions in Salt and Tuff," *Bull. Seism. Soc. Am., 81*, pp. 1272-1291.

Stevens, J. L., N. Rimer, J. R. Murphy and T. G. Barker (1991b), "Simulation of Seismic Signals From Partially Coupled Nuclear Explosions in Spherical and Ellipsoidal Cavities," S-CUBED Technical Report SSS-FR-91-12735.

Prof. Thomas Ahrens
Seismological Lab, 252-21
Division of Geological & Planetary Sciences
California Institute of Technology
Pasadena, CA 91125

Prof. Keiiti Aki
Center for Earth Sciences
University of Southern California
University Park
Los Angeles, CA 90089-0741

Prof. Shelton Alexander
Geosciences Department
403 Deike Building
The Pennsylvania State University
University Park, PA 16802

Dr. Thomas C. Bache, Jr.
Science Applications Int'l Corp.
10260 Campus Point Drive
San Diego, CA 92121 (2 copies)

Prof. Muawia Barazangi
Cornell University
Institute for the Study of the Continent
3126 SNEE Hall
Ithaca, NY 14853

Dr. Douglas R. Baumgardt
ENSCO, Inc
5400 Port Royal Road
Springfield, VA 22151-2388

Dr. T.J. Bennett
S-CUBED
A Division of Maxwell Laboratories
11800 Sunrise Valley Drive, Suite 1212
Reston, VA 22091

Dr. Robert Blandford
AFTAC/TT, Center for Seismic Studies
1300 North 17th Street
Suite 1450
Arlington, VA 22209-2308

Dr. Steven Bratt
ARPA/NMRO
3701 North Fairfax Drive
Arlington, VA 22203-1714

Dale Breding
U.S. Department of Energy
Recipient, IS-20, GA-033
Office of Arms Control
Washington, DC 20585

Dr. Jerry Carter
Center for Seismic Studies
1300 North 17th Street
Suite 1450
Arlington, VA 22209-2308

Mr Robert Cockerham
Arms Control & Disarmament Agency
320 21st Street North West
Room 5741
Washington, DC 20451,

Dr. Zoltan Der
ENSCO, Inc.
5400 Port Royal Road
Springfield, VA 22151-2388

Dr. Stanley K. Dickinson
AFOSR/NM
110 Duncan Avenue
Suite B115
Bolling AFB, DC

Dr Petr Firbas
Institute of Physics of the Earth
Masaryk University Brno
Jecna 29a
612 46 Brno, Czech Republic

Dr. Mark D. Fisk
Mission Research Corporation
735 State Street
P.O. Drawer 719
Santa Barbara, CA 93102

Dr. Cliff Frolich
Institute of Geophysics
8701 North Mopac
Austin, TX 78759

Dr. Holly Given
IGPP, A-025
Scripps Institute of Oceanography
University of California, San Diego
La Jolla, CA 92093

Dr. Jeffrey W. Given
SAIC
10260 Campus Point Drive
San Diego, CA 92121

Dr. Dale Glover
Defense Intelligence Agency
ATTN: ODT-1B
Washington, DC 20301

Dan N. Hagedon
Pacific Northwest Laboratories
Battelle Boulevard
Richland, WA 99352

Dr. James Hannon
Lawrence Livermore National Laboratory
P.O. Box 808, L-205
Livermore, CA 94550

Dr. Roger Hansen
University of Colorado, JSPC
Campus Box 583
Boulder, CO 80309

Prof. David G. Harkrider
Division of Geological & Planetary Sciences
California Institute of Technology
Pasadena, CA 91125

Prof. Danny Harvey
University of Colorado, JSPC
Campus Box 583
Boulder, CO 80309

Prof. Donald V. Helmberger
Division of Geological & Planetary Sciences
California Institute of Technology
Pasadena, CA 91125

Prof. Eugene Herrin
Geophysical Laboratory
Southern Methodist University
Dallas, TX 75275

Prof. Robert B. Herrmann
Department of Earth & Atmospheric Sciences
St. Louis University
St. Louis, MO 63156

Prof. Lane R. Johnson
Seismographic Station
University of California
Berkeley, CA 94720

Prof. Thomas H. Jordan
Department of Earth, Atmospheric &
Planetary Sciences
Massachusetts Institute of Technology
Cambridge, MA 02139

Robert C. Kemerait
ENSCO, Inc.
445 Pineda Court
Melbourne, FL 32940

U.S. Dept of Energy
Max Koontz, NN-20, GA-033
Office of Research and Develop.
1000 Independence Avenue
Washington, DC 20585

Dr. Richard LaCoss
MIT Lincoln Laboratory, M-200B
P.O. Box 73
Lexington, MA 02173-0073

Prof. Charles A. Langston
Geosciences Department
403 Deike Building
The Pennsylvania State University
University Park, PA 16802

Jim Lawson, Chief Geophysicist
Oklahoma Geological Survey
Oklahoma Geophysical Observatory
P.O. Box 8
Leonard, OK 74043-0008

Prof. Thorne Lay
Institute of Tectonics
Earth Science Board
University of California, Santa Cruz
Santa Cruz, CA 95064

Dr. William Leith
U.S. Geological Survey
Mail Stop 928
Reston, VA 22092

Mr. James F. Lewkowicz
Phillips Laboratory/GPE
29 Randolph Road
Hanscom AFB, MA 01731-3010(2 copies)

Dr. Gary McCartor
Department of Physics
Southern Methodist University
Dallas, TX 75275

Prof. Thomas V. McEvilly
Seismographic Station
University of California
Berkeley, CA 94720

Dr. Keith L. McLaughlin
S-CUBED
A Division of Maxwell Laboratory
P.O. Box 1620
La Jolla, CA 92038-1620

Prof. Bernard Minster
IGPP, A-025
Scripps Institute of Oceanography
University of California, San Diego
La Jolla, CA 92093

Prof. Brian J. Mitchell
Department of Earth & Atmospheric Sciences
St. Louis University
St. Louis, MO 63156

Mr. Jack Murphy
S-CUBED
A Division of Maxwell Laboratory
11800 Sunrise Valley Drive, Suite 1212
Reston, VA 22091 (2 Copies)

Dr. Keith K. Nakanishi
Lawrence Livermore National Laboratory
L-025
P.O. Box 808
Livermore, CA 94550

Prof. John A. Orcutt
IGPP, A-025
Scripps Institute of Oceanography
University of California, San Diego
La Jolla, CA 92093

Dr. Howard Patton
Lawrence Livermore National Laboratory
L-025
P.O. Box 808
Livermore, CA 94550

Dr. Frank Pilotte
HQ AFTAC/TT
1030 South Highway A1A
Patrick AFB, FL 32925-3002

Dr. Jay J. Pulli
Radix Systems, Inc.
201 Perry Parkway
Gaithersburg, MD 20877

Prof. Paul G. Richards
Lamont-Doherty Earth Observatory
of Columbia University
Palisades, NY 10964

Mr. Wilmer Rivers
Multimax Inc.
1441 McCormick Drive
Landover, MD 20785

Dr. Alan S. Ryall, Jr.
Lawrence Livermore National Laboratory
L-025
P.O. Box 808
Livermore, CA 94550

Dr.Chandan K. Saikia
Woodward Clyde- Consultants
566 El Dorado Street
Pasadena, CA 91101

Mr. Dogan Seber
Cornell University
Inst. for the Study of the Continent
3130 SNEE Hall
Ithaca, NY 14853-1504

Secretary of the Air Force
(SAFRD)
Washington, DC 20330

Office of the Secretary of Defense
DDR&E
Washington, DC 20330

Thomas J. Sereno, Jr.
Science Application Int'l Corp.
10260 Campus Point Drive
San Diego, CA 92121

Dr. Michael Shore
Defense Nuclear Agency/SPSS
6801 Telegraph Road
Alexandria, VA 22310

Prof. David G. Simpson
IRIS, Inc.
1616 North Fort Myer Drive
Suite 1050
Arlington, VA 22209

Dr. Jeffrey Stevens
S-CUBED
A Division of Maxwell Laboratory
P.O. Box 1620
La Jolla, CA 92038-1620

Prof. Brian Stump
Los Alamos National Laboratory
EES-3
Mail Stop C-335
Los Alamos, NM 87545

Prof. Tuncay Taymaz
Istanbul Technical University
Dept. of Geophysical Engineering
Mining Faculty
Maslak-80626, Istanbul Turkey

Prof. M. Nafi Toksoz
Earth Resources Lab
Massachusetts Institute of Technology
42 Carleton Street
Cambridge, MA 02142

Dr. Larry Turnbull
CIA-OSWR/NED
Washington, DC 20505

Dr. Karl Veith
EG&G
5211 Auth Road
Suite 240
Suitland, MD 20746

Prof. Terry C. Wallace
Department of Geosciences
Building #77
University of Arizona
Tuscon, AZ 85721

Dr. William Wortman
Mission Research Corporation
8560 Cinderbed Road
Suite 700
Newington, VA 22122

ARPA, OASB/Library
3701 North Fairfax Drive
Arlington, VA 22203-1714

HQ DNA
ATTN: Technical Library
Washington, DC 20305

Defense Technical Information Center
Cameron Station
Alexandria, VA 22314 (2 Copies)

TACTEC
Battelle Memorial Institute
505 King Avenue
Columbus, OH 43201 (Final Report)

Phillips Laboratory
ATTN: GPE
29 Randolph Road
Hanscom AFB, MA 01731-3010

Phillips Laboratory
ATTN: TSML
5 Wright Street
Hanscom AFB, MA 01731-3004

Phillips Laboratory
ATTN: PL/SUL
3550 Aberdeen Ave SE
Kirtland, NM 87117-5776 (2 copies)

Dr. Michel Campillo
Observatoire de Grenoble
I.R.I.G.M.-B.P. 53
38041 Grenoble, FRANCE

Dr. Kin Yip Chun
Geophysics Division
Physics Department
University of Toronto
Ontario, CANADA

Prof. Hans-Peter Harjes
Institute for Geophysic
Ruhr University/Bochum
P.O. Box 102148
4630 Bochum 1, GERMANY

Prof. Eystein Husebye
NTNF/NORSAR
P.O. Box 51
N-2007 Kjeller, NORWAY

David Jepsen
Acting Head, Nuclear Monitoring Section
Bureau of Mineral Resources
Geology and Geophysics
G.P.O. Box 378, Canberra, AUSTRALIA

Ms. Eva Johannisson
Senior Research Officer
FOA
S-172 90 Sundbyberg, SWEDEN

Dr. Peter Marshall
Procurement Executive
Ministry of Defense
Blacknest, Brimpton
Reading FG7-FRS, UNITED KINGDOM

Dr. Bernard Massinon, Dr. Pierre Mechler
Societe Radiomana
27 rue Claude Bernard
75005 Paris, FRANCE (2 Copies)

Dr. Svein Mykkeltveit
NTNT/NORSAR
P.O. Box 51
N-2007 Kjeller, NORWAY (3 Copies)

Dr. Jorg Schlittenhardt
Federal Institute for Geosciences & Nat'l Res.
Postfach 510153
D-30631 Hannover , GERMANY

Dr. Johannes Schweitzer
Institute of Geophysics
Ruhr University/Bochum
P.O. Box 1102148
4360 Bochum 1, GERMANY

Trust & Verify
VERTIC
Carrara House
20 Embankment Place
London WC2N 6NN, ENGLAND